In vitro myogenesis in skeletal muscle cells from type 2 diabetic and non-diabetic subjects

Comparison of metabolic properties, mitochondrial content and mass, ATP concentration and differentiation capacity

Dissertation for the degree of Master of Pharmacy

Lene Hjelle

Department of Pharmaceutical Bioscience,
School of Pharmacy,
Faculty of Mathematics and Natural Sciences,
University of Oslo

Department of Skeletal Muscle Physiology,
The Pennington Biomedical Research Center,
Louisiana State University

May 2011

In vitro myogenesis in skeletal muscle cells from type 2 diabetic and non-diabetic subjects

Comparison of metabolic properties, mitochondrial content and mass, ATP concentration and differentiation capacity

Lene Hjelle

Dissertation for the degree of Master of Pharmacy

Department of Pharmaceutical Bioscience,
School of Pharmacy,
Faculty of Mathematics and Natural Sciences,
University of Oslo

Department of Skeletal Muscle Physiology,
The Pennington Biomedical Research Center,
Louisiana State University

May 2011

Supervisors
Eric Ravussin, PhD
Arild Chr. Rustan, PhD

Acknowledgements

The research for this master's thesis was conducted at the Pennington Biomedical Research Center (PBRC), Baton Rouge, USA from July 2010 – March 2011.

First of all I want to give my sincere gratitude to Dr. Eric Ravussin for giving me the opportunity to come to PBRC and conduct research for my master's thesis. Thank you for all your good advice and interesting discussions.

My gratitude is also sent to Jeffrey Covington, Dr. Sudip Bajpeyi, Ph.D., Dr. Virgile LeCoultre and the rest of the Skeletal Muscle lab for guidance and advice as well as informative and interesting discussions throughout the year.

Many thanks go to Dr. Krisztian Stadler and Dr. Jose Galgani for helpful input and discussions.

Pamela Rogers is thanked for excellent training in using the "Seahorse machine" and help with my work in the lab.

I would also like to thank my supervisor at the University of Oslo, Professor Arild Chr. Rustan for help and guidance during the writing process.

Lene Hjelle,

Oslo, May 2011

Table of contents

Abstract

Diabetes mellitus is a metabolic disorder resulting from defective insulin secretion, impaired insulin action or both. The consequence of this is chronic hyperglycemia with disturbance of carbohydrate, fat and protein metabolism. The prevalence of diabetes, especially type 2 diabetes (T2D), is rapidly increasing throughout the world, parallel to this; we also see an increase in the obesity epidemic. The mechanisms underlying the metabolic defects of T2D and obesity are still largely unknown, but there are several studies indicating a strong association between insulin resistance, increased lipid accumulation and impaired fat oxidation in insulin sensitive tissues. Muscular mitochondrial dysfunction has been proposed as an underlying cause to the metabolic disorders, due to observations of reduced mitochondrial oxidative capacity and number in skeletal muscle of insulin resistant and T2D individuals.

The purpose of this study was to determine possible differences in metabolic properties between skeletal muscle cells from T2D and non-diabetic (N-D) subjects. Secondly, it was of interest to assess mitochondrial measures (i.e. mitochondrial content and mass, ATP concentration and OXPHOS content) and MHC content (differentiation marker) in muscle cells from the two donor groups. This was done in order to test the hypothesis of whether a possible impairment in metabolic properties in skeletal muscle of T2D individuals, could be caused by a lower mitochondrial activity/number or by an impaired differentiation capacity of myoblasts.

Muscle biopsies from 10 obese, T2D patients and 10 lean, healthy control subjects were obtained at baseline (pre-intervention). Metabolic properties of myoblasts and myotubes, from the two donor groups were evaluated by measuring rates of oxygen consumption (OCR) and extracellular acidification (ECAR) in an XF24 Analyzer. Mitochondrial content and mass were measured by rt-PCR and mitotracker, respectively. ATP concentration was determined by the EnzyLight ATP assay kit, while OXPHOS and MHC content were determined by Western immunoblotting.

Results showed that the skeletal muscle cells, established from obese, T2D subjects, had a substantially reduction in OCR and ECAR compared with cells from the control group. Measurements of mitochondrial mass and content, ATP concentration and OXPHOS content were not different between cells from the two groups. The MHC content was significantly lower in myotubes from T2D individuals compared to cells from the control group. These results may indicate an impaired mitochondrial function in T2D cells, rather than a lower mitochondrial number. However, the reduction in OCR and ECAR seen in T2D subjects could simply be caused by less differentiated myotubes in this group.

Abbreviations

ACBP	Acyl-CoA binding protein
ADP	Adenosine diphosphate
ATP	Adenosine triphosphate
AU	Arbitrary units
BMI	Body mass index
BSA	Bovine serum albumin
CLB	Cell lysis buffer
CO_2	Carbon dioxide
CytC	Cytochrome C
DAPI	4',6-Diamidino-2-phenylindole dihydrochloride
ddH_2O	Double distilled water
DMEM	Dulbecco's modified Eagle medium
DMSO	Dimethyl sulfoxide
DPBS	Dulbecco's phosphate buffered saline
e^-	Electron
ECAR	Extracellular acidification rate
ECL	Enhanced chemiluminescence
EDTA	Ethylenediaminetetraacetic acid
ETC	Electron transport chain
FABP	Fatty acid binding protein
FADH	Flavine adenine dinuclotide H^+
FBS	Fetal bovine serum
FCCP	Carbonyl cyanide-p-trifluoromethoxyphenylhydrazone
FFA	Free fatty acid
GAPDH	Glyceraldehyde-3-phosphate dehydrogenase
GLUT	Glucose transporter
H^+	Proton
HBSS	Hank's balanced salt solution
HuEGF	Human epidermal growth factor
IOD	International optical density
IRS	Insulin receptor substrate
MAG	Monoacylglycerol
MB	Myoblast(s)
αMEM	Minimum essential medium alpha
MHC	Myosin heavy chain
MRF	Myogenic regulatory factor(s)

MT	Myotube(s)
mtDNA	Mitochondrial DNA
NADH	Nicotinamide adenine dinuclotide H^+
N-D	Non-diabetic(s)
ND1	NADH dehydrogenase subunit 1
ND4	NADH dehydrogenase subunit 2
O_2	Oxygen
OCR	Oxygen consumption rate
OXPHOS	Oxidative phosphorylation
PAG	Phosphoglyceraldehyde
PBRC	Pennington Biomedical Research Center
PDK-1	3-Phosphoinositide-dependent protein kinase 1
PI3K	Phosphatidylinositol-3 kinase
PIP_2	Phosphatidylinositol (4,5)-biphosphate
PIP_3	Phosphatidylinositol (3,4,5)-triphosphate
PKB	Protein kinase B (Akt)
RCF	Relative centrifugal force
RIPA	Radioimmunoprecipitation assay
RPM	Revolutions per minute
RQ	Respiratory quotient
S.E.M	Standard error of mean
T2D	Type 2 diabetic(s)
TAG	Triacylglycerol
TCA^1	Tricarboxylic acid cycle
TCA^2	Trichloroacetic acid
UQ	Ubiquinone
VO_{2max}	Maximal oxygen consumption
WHO	World Health Organization
XF	Extracellular flux

1 Introduction

1.1 Type 2 diabetes

Diabetes mellitus is defined as a metabolic disorder of multiple etiology, characterized by chronic hyperglycemia, with disturbances of carbohydrate, fat and protein metabolism resulting from defects in insulin secretion, insulin action, or both[1]. This disease has become an increasing problem worldwide, and numbers from the World Health Organization (WHO) show that more than 220 million people had diabetes in 2009[2]. The two most common forms of diabetes are type 1 and type 2 (T2D). WHO has estimated that 90 % of people with diabetes have T2D[2]. Patients with type 1 diabetes have deficient insulin production, and require daily administration of insulin. T2D is mostly associated with insulin resistance, eventually leading to insufficient insulin production. Untreated T2D is often characterized by elevated levels of fasting blood glucose in addition to elevated levels of insulin. This is a compensation mechanism in which the body attempts to produce more insulin to overcome the elevated levels of blood glucose. Hyperglycemia occurs when insulin has an impaired effect in liver, muscle and adipose tissue.

Hyperglycemia over time damages both the blood vessels and the internal organs. Macrovascular complications such as cardiovascular disease and stroke are often associated with T2D. In addition, there are several microvascular complications such as microangiopathy in the eyes, kidneys and nerves[3]. An estimate from 2005 showed that 1.1 million people died from diabetes[2]. This number is most likely to be much larger since a lot of deaths in diabetes patients are recorded as heart disease or kidney failure, both common complications of diabetes.

T2D can be ameliorated pharmacologically with oral antidiabetics, incretins and insulin. Oral antidiabetics have various mechanisms of action, sulphonylureas and glinides increase β-cell insulin output, biguanides decrease liver glucose output, glitazones reduce insulin resistance in muscle, adipose tissue and liver and α-glucosidase inhibitors delay absorption of glucose form the intestine.

Incretins and insulin are available as injectable agents that act by increasing the production of insulin (incretins) or substituting insulin (insulin and insulin analogues)[4]. Although there are several pharmacological treatments for the disease, alterations in diet, increased physical activity, weight loss and smoking cessation still remain important lifestyle changes beneficial for the treatment of diabetes.

1.2 Insulin resistance in skeletal muscle

The development of diabetes involves several pathogenic processes, including destruction of the pancreatic β-cells with consequent insulin deficiency, and other processes that result in resistance to insulin action. Deficient action of insulin on target tissues, due to insensitivity or lack of insulin, leads to abnormalities in carbohydrate, fat and protein metabolism. The molecular mechanisms that underlie the metabolic impairments of T2D are still largely unknown. However, it appears that genetic predisposition and environmental factors both play an important role in the onset and risk for development of the disease[5, 6].

Whole-body glucose homeostasis is largely affected by the skeletal muscle's insulin-sensitivity (or lack of sensitivity) [7]. This organ is considered the most important glucose absorptive organ, and has, therefore, long been considered one of the primary targets for understanding mechanisms for development of insulin resistance and T2D. In healthy individuals, skeletal muscle accounts for more than 70 % of whole-body insulin stimulated glucose uptake [8-10]. However, in normal-weight subjects with insulin resistance, total body glucose metabolism can be reduced by ~40 %[10].

One of the key characteristics of T2D is insulin resistance, in addition to several abnormalities in the biological response to insulin including; decreased glucose transport, glucose oxidation and glycogen synthesis[11]. In turn, insulin resistance is mostly determined by increased intramyocellular lipid accumulation and reduced muscle fat oxidation [9, 12-14]. Several studies have also observed lower mitochondrial number and activity in these individuals [15]. In 2008, Turner and Heilbronn[16] published a complete summary of the differences between insulin-resistant and -sensitive individuals. Based on these findings, it was postulated that mitochondrial dysfunction would limit the capacity to

match fatty acid oxidation to fatty acid (over) supply, leading to increased muscle lipid accumulation and insulin resistance[13].

1.3 Glucose and lipid metabolism

The human body switches between two phases of energy utilization; the post-absorptive phase and the postprandial phase. In the post-absorptive phase the cells utilize the energy coming mostly from the nutrients being mobilized from the body's energy stores. In the postprandial phase, energy substrates are coming mostly from the food recently ingested. Since meals are short and periods of fast are much longer, the body has to rely on an efficient storage of incoming food as glycogen (i.e. glucose), triglycerides (i.e. fat) and proteins (i.e. amino acids).

The skeletal muscle is the main organ for oxidation of glucose and lipids[17, 18], and it comprises about 40 % of body weight in non-obese subjects[19]. After a meal (postprandial phase), the insulin level rises, which in turn leads to increased glucose metabolism and utilization. Fatty acid oxidation, on the other hand, will exceed storage during the fasting state (post-absorptive phase). This shift in energy utilization is referred to as metabolic flexibility, and it is important that the skeletal muscle can adapt to these two opposite physiological conditions[20].

1.3.1 Glucose metabolism

Glucose is transported into muscle cells through glucose transporter (GLUT) proteins, found in different tissues of the body. Each isoform of the GLUT proteins play a specific role in the glucose metabolism[21]. Several of these proteins are expressed in skeletal muscle, but it is mainly the GLUT4 isoform that is modulated by insulin and muscle contraction[17].

Activation of the insulin receptor triggers a signaling cascade which leads to the translocation of GLUT4 to the cell membrane[17] (figure 1.1). When insulin binds to its receptor's extracellular α-subunit, this leads to autophosphorylation of the transmembrane β-

subunit, which in turn will lead to the phosphorylation of the insulin receptor substrate (IRS). Phosphorylated IRS interacts with Scr-homology-2 (SH2) domains which further activate the phosphatidylinositol-3 kinase (PI3K)[22]. Activated PI3K will further activate downstream proteins like phosphatidylinositol(3,4,5)-triphosphate (PIP_3),3-phosphoinositide dependent protein kinase-1 (PDK1) and protein kinase B (Akt/PKB), which results in translocation of GLUT4[17, 22].

When the insulin concentration increases, the number of GLUT4 proteins in the cell membrane also increases, and this will in turn lead to an increase in the glucose transport capacity into muscle. Once glucose has been taken up by the GLUT proteins in the cell membrane, it is phosphorylated by hexokinase to glucose-6-phosphate. In turn, glucose-6-phosphate can either be utilized in the glycolytic pathway, glycolysis, or be incorporated into glycogen by glycogen synthase. In some cases, glucose can be stored as fat via *de novo* lipogenesis[9] (figure 1.2).

Most of the changes in glucose metabolism seen in patients with T2D are due to the skeletal muscle and liver's transition to an insulin resistant state. Several studies have shown that the skeletal muscle of insulin resistant subjects shows surprisingly normal GLUT4 expression. This may indicate an impaired translocation of GLUT4 from intracellular stores to the plasma membrane, thus causing insulin's reduced ability to stimulate glucose uptake[23]. There are also several studies on glucose uptake in muscle that have shown reduced activity in insulin receptor substrate-1 (IRS-1) phosphorylation and PI3K activity in insulin resistant skeletal muscle of obese and T2D patients[24, 25]. These findings support the hypothesis of an impaired translocation of GLUT4, as these intermediates are essential in this process.

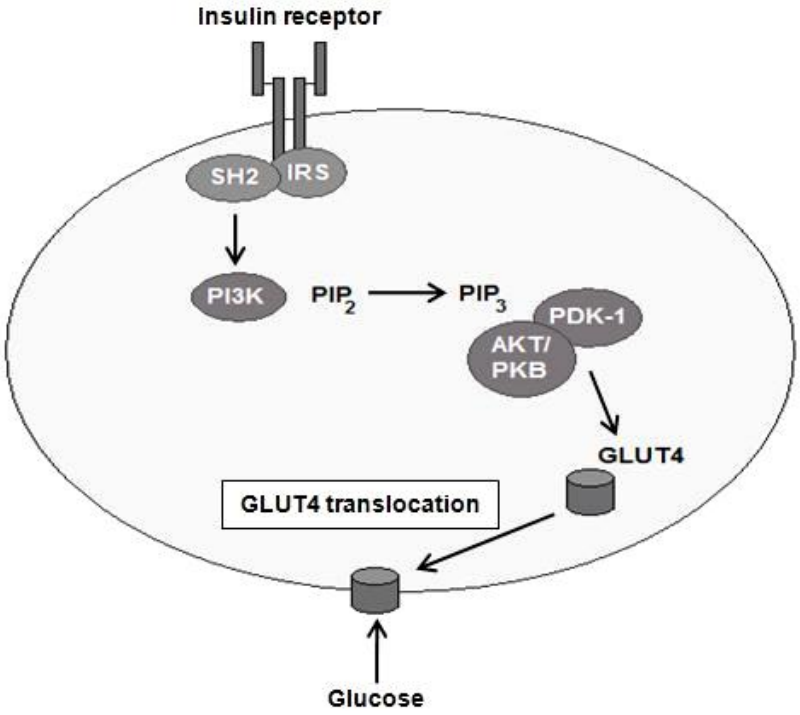

Figure 1.1: Simplified overview of glucose uptake. Insulin binds to the α-subunit of its receptor. This triggers a downstream cascade, which leads to translocation of GLUT4 to the plasma membrane. Akt/PKB; protein kinase B, IRS; insulin receptor substrate, PDK-1; 3-phosphoinositide dependent protein kinase-1, PIP_2; phosphatidylinositol (4,5)-biphosphate, PIP_3; phosphatidylinositol (3,4,5)-triphosphate, PI3K; phosphatidylinositol-3 kinase, SH2; Scr-homology-2. Figure modified from Tremblay et al. [17]

1.3.2 Lipid metabolism

The fat we ingest through our food is usually in the form of triacylglycerols (TAG). In the intestine, TAG is broken down to free-fatty acids (FFA) and monoacylglycerol (MAG), by the pancreatic lipases[26, 27]. FFAs are taken up into cells by fatty acid transporters in the plasma membrane (i.e. CD36/FAT) (figure 1.2). In the cytosol, the FFAs are transported intracellularly by fatty acid binding proteins (FABP) and converted to acyl-CoA by acyl-CoA synthase. The acyl-CoA binding protein (ACBP) transports acyl-CoA to mitochondria or peroxisomes, where they undergo β-oxidation resulting in ATP production and heat generation. Acyl-CoA can also undergo esterification in the endoplasmatic reticulum where they form new lipids (i.e. phospholipids, triacylglycerols and various cholesteryl esters)[28].

Several studies have shown that insulin resistance in skeletal muscle is associated with reduced lipid oxidation and lipid accumulation. A study conducted by Kelley and Simoneau [29] demonstrated that T2D patients had reduced lipid oxidation rates during the post-absorptive phase. Moreover, Mensink *et al*. [30] showed that patients with impaired glucose tolerance also had reduced uptake and oxidation of FFAs, while Krssak *et al.* [31] showed an inverse correlation between insulin stimulated whole-body glucose uptake and intramyocellular lipid content. These studies, and others, have led to the hypothesis of a mitochondrial dysfunction which drives impaired fat oxidation and consequently lipid accumulation and insulin resistance[9].

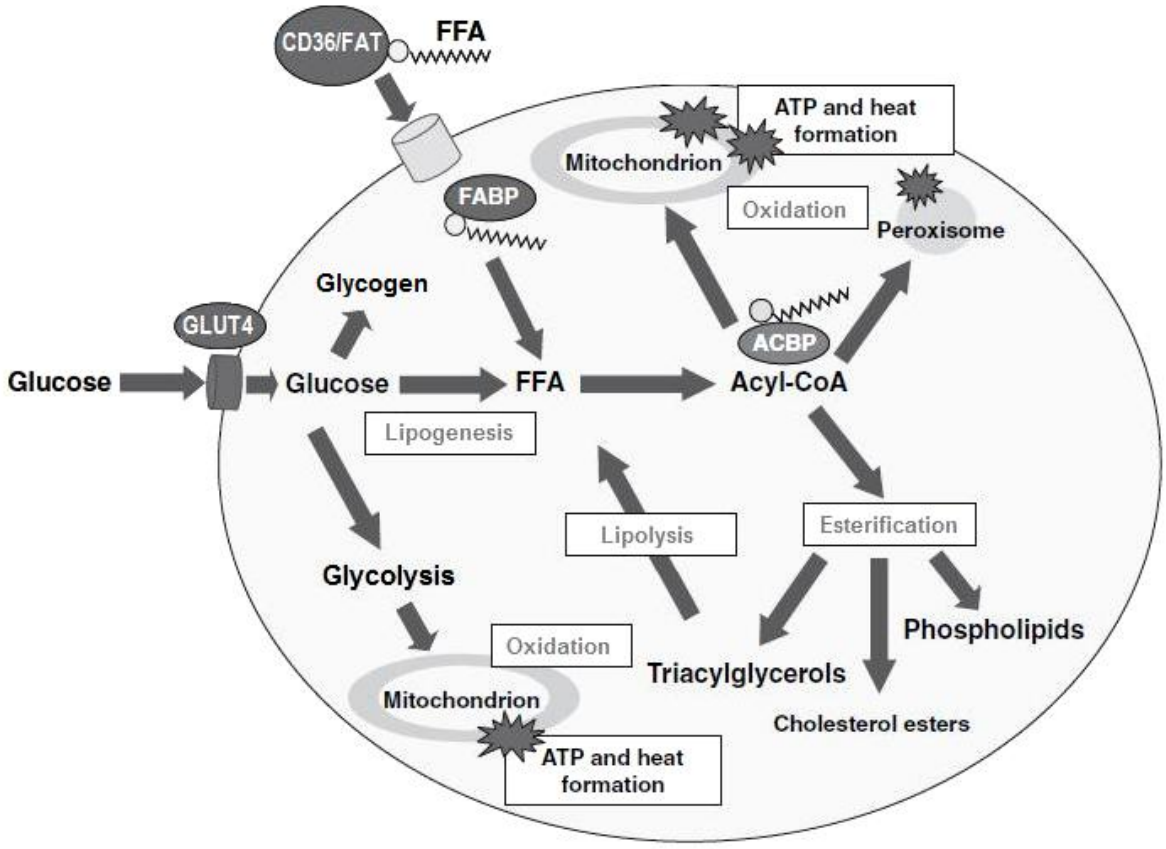

Figure 1.2: Simplified overview of glucose and lipid metabolism. ACBP; acyl-CoA binding protein, ATP; adenosine triphosphate, CD36/FAT; fatty acid transporter, FABP; fatty acid binding protein, FFA; free fatty acid, GLUT4; glucose transporter 4. Figure modified from Aas et al[28]

1.4 Metabolic flexibility

Metabolic flexibility is the skeletal muscle's ability to switch between fatty-acid oxidation during fasting to insulin stimulated glucose oxidation after a meal (postprandial phase) (figure 1.3). Skeletal muscle of healthy, lean subjects is characterized by metabolic flexibility, while we see a loss or impairment of this phenomenon in obese, insulin resistant individuals and even more so in T2D subjects [20, 32, 33]. Conditions such as these are often associated with reduced lipid oxidation during fasting, impaired postprandial switch from lipid to glucose oxidation and reduced capacity to increase lipid oxidation during exercise. This loss or impairment is often referred to as metabolic inflexibility[34].

The respiratory quotient (RQ) is an important tool for the assessment of metabolic flexibility. The RQ is the ratio between CO_2 production and O_2 consumption *in vivo*, and this ratio reflects the mixture of fuels used by the body (i.e. glucose and lipids)[35]. During the postprandial phase, where glucose is the main energy source, the RQ is approximately 1. Switching to the fasting phase will give a lower RQ, due to the consumption of a great deal more O_2 relative to the production of CO_2 during fat metabolism. A relatively low fat oxidation is indicated by a high RQ, which can predispose to increased body fat storage. A low RQ, on the other hand, could represent a protective marker against overweight[35, 36]. During the transition from the fed to the overnight-fasted conditions, fatty acids are the main readily available energy source, which is indicated by a progressive fall in RQ during the night. Metabolic inflexibility to lipids may be defined as an impaired drop in RQ during an overnight fast (high fasting RQ)[20]. Several studies have suggested an elevated fasting RQ in skeletal muscle from obese, insulin resistant and T2D subjects [15, 29, 37].

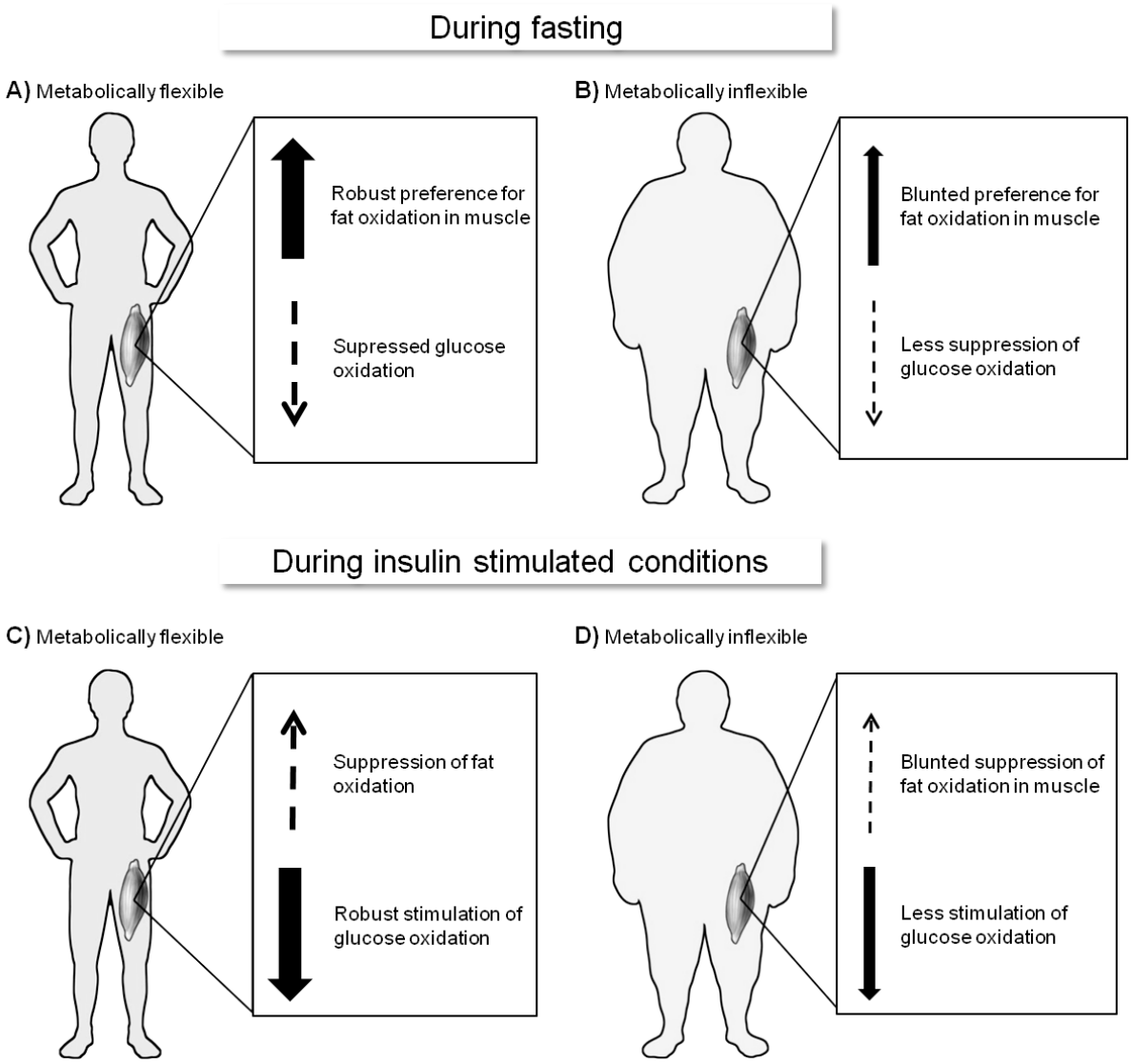

Figure 1.3: Metabolic flexibility in skeletal muscle. During fasting, **A)** metabolic flexible individuals have a robust preference for fatty acid oxidation; while glucose oxidation is being suppressed, **B)** metabolic inflexible individuals, on the other hand, rely less upon fatty acid oxidation, while there is a reduced suppression of glucose oxidation. During insulin stimulated conditions after a meal, **C)** metabolic flexible individuals have a robust stimulation of glucose oxidation, while fatty acid oxidation is being suppressed, **D)** metabolic inflexible individuals, on the other hand, will have less stimulation of glucose oxidation and blunted suppression of fatty acid oxidation. Figure from Kelley et al.[32]

1.5 Human skeletal muscle development and muscle cells

The skeletal muscle is, as previously mentioned, an important target for understanding the mechanisms behind the development of insulin resistance and T2D. The *in vitro* cell culture model is of great importance in this research field, as it provides a unique opportunity to

assess scientific hypothesis. It has been demonstrated that primary myotubes, grown from satellite cells (collected by muscle biopsy), conserve the diabetic phenotype of diabetic donors[38, 39], suggesting that such a cell culture system represents an ideal tool to understand the mechanisms of insulin resistance.

The skeletal muscle consists of elongated muscle cells, called myotubes (figure 1.4 B, D). These muscle cells are formed during fetal development by the fusion of committed muscle cell precursors, myoblasts, (figure 1.4 A, C) in a process called myogenesis (figure 1.5). Due to this fusion, the myotubes contain multiple nuclei within each cell. The myoblasts proliferate, without differentiation, as long as particular growth factors are present. As soon as these factors are depleted, the myoblasts leave the cell cycle and the differentiation, with the synthesis of muscle specific proteins (e.g. myosin and tropomyosin), begins[40].

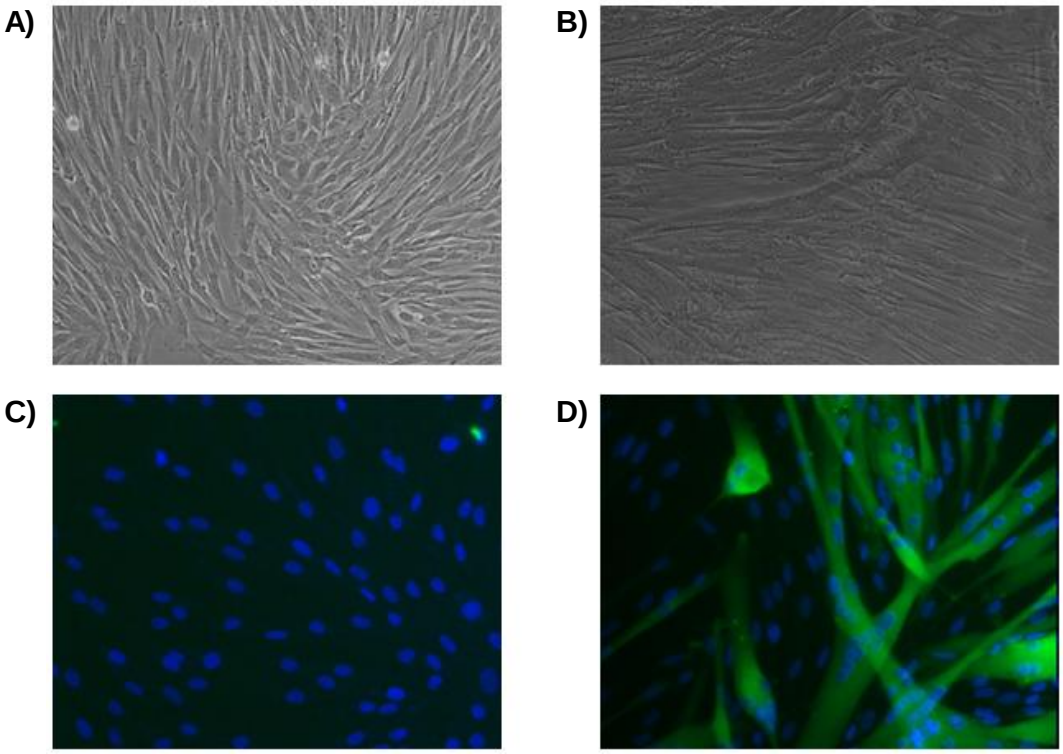

Figure 1.4: Human skeletal muscle differentiation. CD56+ cells (myoblasts) were cultured in growth medium at 37°C in a humidified atmosphere containing 5 % CO_2. At ~80 % confluence, myoblasts were induced to differentiate by changing medium (differentiation medium). Light microscope images of **A)** myoblasts, pre-differentiation and **B)** myotubes, 5 days post-differentiation. Staining images with **C)** DAPI stain of the nuclei and **D)** DAPI stain of the nuclei and antimyocin stain of the myotubes. (Staining images from previous experiments conducted by Pamela Rogers at the Pennington Biomedical Research Center, Ravussin lab).

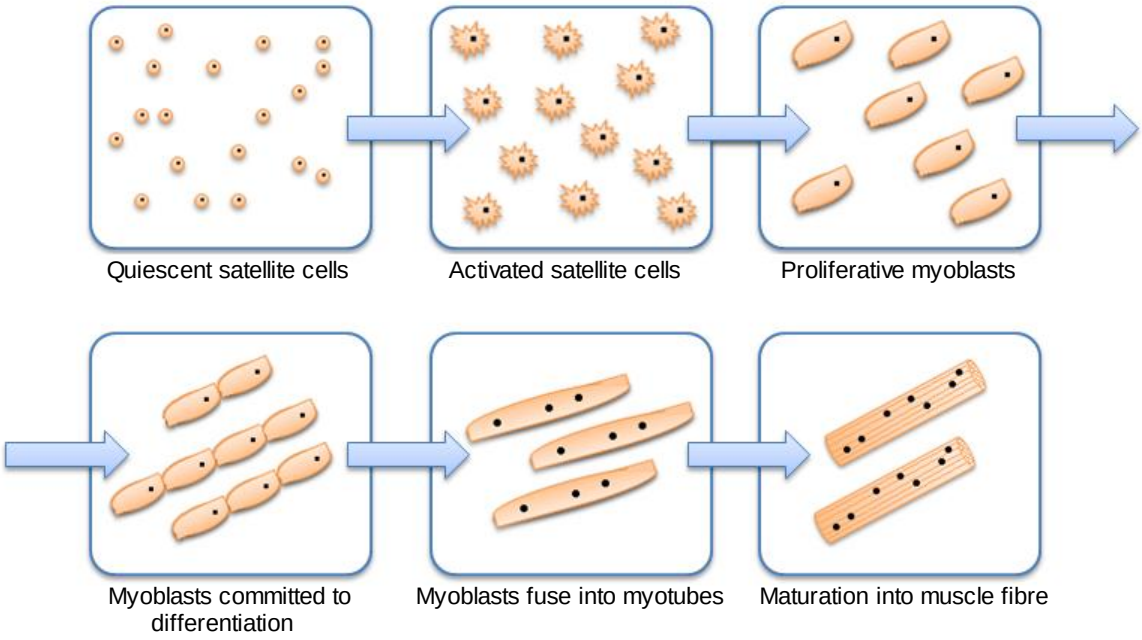

Figure 1.5: Skeletal muscle cell development from quiescent satellite cells to mature muscle fibers. In the proliferation state, committed myoblasts divide in the presence of growth factors. When the growth factors are depleted, the proliferation state stops, and the myoblasts start to fuse into myotubes. The myotubes then become organized into muscle fibers. Figure modified from Gilbert, and Zammit et al [40, 41]

1.5.1 The myogenic regulatory factors

There are several myogenic regulatory factors (MRFs) involved in myogenesis. The MRFs, also referred to as the MyoD family, are specific for muscle cells. These proteins all bind to similar sites on the DNA to activate muscle specific genes. The family consists of; MyoD, Myf5, Myogenin and MRF4[41]. The MRFs can be divided into two groups; the primary MRFs (MyoD and Myf-5) and the secondary MRFs (myogenin and MRF4). The primary MRFs are important in the determination step, where proliferating somatic cells commit to the myogenic lineage, while the secondary MRFs are important in the differentiation step, where the myoblasts fuse into myotubes, which eventually become organized into muscle fibers[42].

1.5.2 Myosin heavy chain (MHC)

The myosins are part of another important muscle specific protein family. This family consists of ATP-dependent motor proteins, which play an essential role in muscle contraction. The interior of the muscle fibers are densely packed with myofibrils, which mainly consist of two types of myofilaments. The myofilaments are thin "threads" that are made up of the proteins; actin and myosin[26]. Remels et al[43] has previously shown that myotubes express significant amounts of MHC (both fast, type II, and slow, type I), while myoblasts express extremely low levels of both MHCs.

1.6 Mitochondria

1.6.1 Mitochondrial function and content

The mitochondria are oval shaped organelles found in most eukaryotic cells. Each mitochondrion has a unique genome in the form of circular mitochondrial DNA (mtDNA)[27, 44]. The mitochondria are made up of two membranes, an outer membrane and an inner membrane, which create two mitochondrial compartments; an internal space called the matrix and an intermembrane space, between the outer and the inner membrane. The outer membrane is permeable to all molecules of 5000 Daltons or less, unlike the inner membrane, which is highly impermeable to all molecules. The inner membrane consists of numerous folds which create a large surface; here we find several proteins with three important functions; (1) proteins that are responsible for the oxidation reactions in the electron transport chain (ETC), (2) the ATP synthase, responsible for the production of ATP and (3) transport proteins[27]. The most prominent roles of mitochondria are to produce ATP through respiration (i.e. phosphorylation of ADP), and they are responsible for approximately 90 % of cellular ATP production[26]. This process of cellular respiration, also known as aerobic respiration, is dependent on the presence of oxygen. The number of mitochondria within a cell can vary from a few mitochondria per cell to several thousands, depending on the energy turnover within the cell[27].

1.6.2 Mitochondria's role in T2D

The skeletal muscle is known to have a high energy turnover and, therefore, a large number of mitochondria per cell[45]. Metabolic flexibility is, as mentioned earlier, the ability the skeletal muscle has to switch from fatty acid oxidation in the fasting state, to insulin-stimulated glucose oxidation after a meal. An important component of insulin resistance appears to be a decreased ability of insulin to regulate fuel utilization. This impaired ability to switch from lipid to carbohydrate oxidation in response to insulin, is often referred to as metabolic inflexibility[34]. These findings have led to an increased interest in the mitochondria and the skeletal muscle when it comes to research in diabetes. Recently, several studies have indicated that mitochondrial dysfunction may play an important role in the pathogenesis of insulin resistance and T2D [45-47].

A study conducted by Kelley and Simoneau[29] demonstrated a decreased leg lipid oxidation in obese and T2D subjects. Several studies have also shown a strong negative correlation between lipid oxidation and insulin resistance [15, 48, 49]. Kelley et al[45] demonstrated that muscle mitochondria, established from obese T2D patients, had reduced oxidative capacity compared with the lean control group. Moreover, the study showed that the morphology of mitochondria from obese and T2D subjects were altered, showing significantly smaller mitochondria in these two groups compared with the lean control group. Patti *et al*[50]looked at gene expression in skeletal muscle of T2D and non-diabetic subjects. The study showed that the expression of several genes involved in fatty acid oxidation, glycolysis and the TCA cycle was significantly reduced in T2D subjects compared to the control group. This was also true for the expression of several genes involved in the ETC, where subunits of complex I-IV and subunits of the ATP synthase were decreased in T2D subjects.

1.6.3 Cellular metabolism

Cellular metabolism is the process of substrate uptake (i.e. oxygen, glucose, fatty acids and proteins) and energy conversion through a series of enzymatically controlled oxidation and reduction reactions. These reactions are executed through a series of intracellular biochemical processes (glycolysis, the TCA cycle, the ETC and oxidative phosphorylation) which result in the production of ATP and the release of heat and chemical byproducts (lactate and CO_2) into the extracellular environment.

Glycolysis and the TCA cycle

Glycolysis, which occurs in the cytosol, is the conversion of glucose to two molecules of pyruvic acid (figure 1.6 A). During this process two ATP molecules are formed, in addition to NADH, which acts as an electron donor in the ETC. The pyruvic acid produced by glycolysis is rapidly decarboxylated to form CO_2 (waste product), NADH (to the ETC) and acetyl-CoA, which enters the TCA cycle within the mitochondria (figure 1.6 B). The TCA cycle produces ATP and reduced coenzymes (NADH and FADH), which enters the ETC. ATP formed during glycolysis is not dependent on O_2, and although the TCA cycle itself does not use O_2, it requires O_2 to proceed[27]. Under anaerobic conditions (lack of O_2), pyruvic acid is converted into lactic acid.

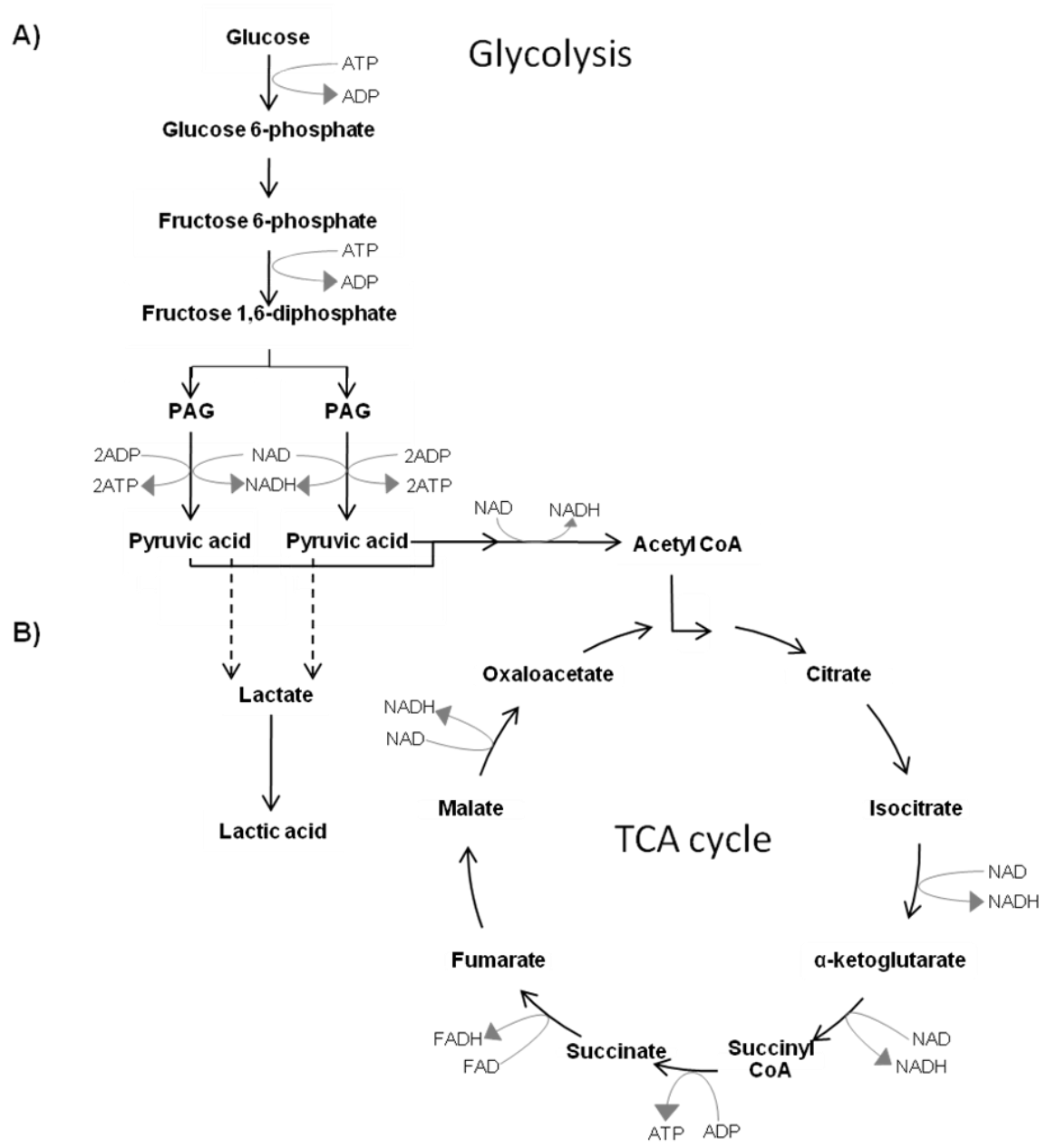

Figure 1.6: Schematic overview of glycolysis and the TCA cycle. A) Glycolysis and **B)** the TCA cycle. ADP; adenosine diphosphate, ATP; adenosine triphosphate, FADH; flavin adenine dinucleotide H^+, NADH; Nicotinamide adenine dinucleotide H^+, PAG; phosphoglyceraldehyde, TCA; tricarboxylic acid cycle.

The electron transport chain (ETC) and oxidative phosphorylation

The ETC is a collection of protein complexes embedded in the mitochondrial inner membrane. It consists of three proton pumps (NADH dehydrogenase = complex I, cytochrome *c* reductase = complex III, and cytochrome *c* oxidase = complex IV) and an enzyme complex not pumping protons (succinate dehydrogenase = complex II)[51] (figure 1.7). The electrons are transferred from complex to complex along the ETC, which is an energetically producing process. The spontaneous electron flow through the complexes are coupled to the non-spontaneous H^+ ejection from the mitochondrial matrix, which creates a membrane potential and a pH gradient across the mitochondrial inner membrane. The first complex of the ETC receives electrons from NADH, and the last complex transfers electrons to molecular oxygen. In this latter process oxygen ions (O^{2-}) are formed, and these will immediately react with hydrogen ions (H^+), within the mitochondrial matrix, to form the final product, water (H_2O). The strongly electronegative oxygen atoms in the oxygen molecule are, in other words, the final recipient of the electrons, which means that the ETC would come to a halt without oxygen[26, 27].

The ETC is coupled to the ATP synthase, a reversible proton pump, which uses the energy of the proton gradient across the inner mitochondrial membrane to synthesize ATP[51] (figure 1.7). The ATP synthase consists of a catalytic subunit (F_1) and a membrane subunit (F_0), that mediates proton transport[52, 53]. The proton gradient created by the ETC makes it energetically favorable for protons to flow back into the matrix. The ATP synthase creates a hydrophilic pathway across the mitochondrial inner membrane allowing protons to flow down their electrochemical gradient, which drives the energetically unfavorable reaction of ADP and Pi to form ATP[27].

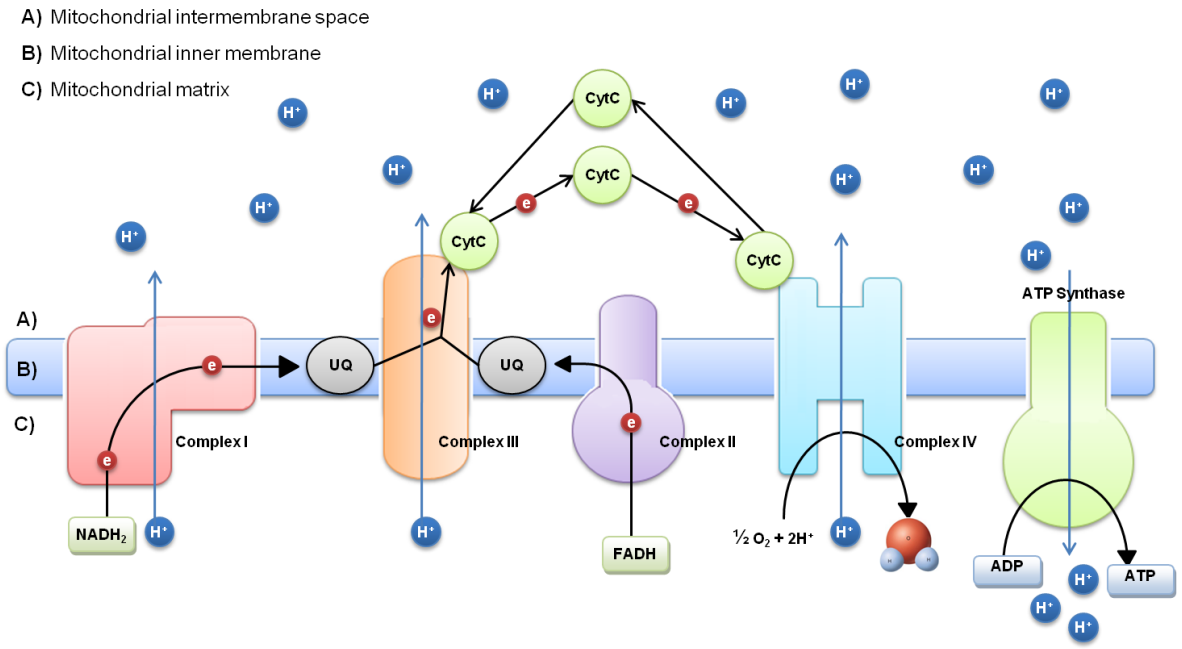

Figure 1.7: The electron transport chain (ETC) and oxidative phosphorylation through the ATP synthase. NADH and FADH, from glycolysis and the TCA cycle, donates electrons, which are being transported through the complexes in the ETC. Meanwhile, protons are transported over the mitochondrial inner membrane and out of the matrix. This creates a proton gradient, which in turn leads to the production of ATP by phosphorylation of ADP. ADP; adenosine diphosphate, ATP; adenosine triphosphate, CytC; cytochrome C, e^-; electron, FADH; flavine adenine dinucleotide H^+, H^+; proton, H_2O; water, NADH; nicotinamide adenine dinucleotide H^+, O_2; oxygen, UQ; ubiquinone.

1.7 Substances used to measure mitochondrial function

1.7.1 Oligomycin

The oligomycins are members of a family of macrolide spiroketal antibiotics that were first identified in a strain of *Streptomyces diastatochromogesnes*[54]. These compounds act by binding to the F_0 subunit of the ATP synthase and consequently block this proton channel. The inhibition of the ATP synthase will lead to reduced ATP production and a halt in the electron transport chain [54, 55], which in turn leads to a reduction in O_2 consumption.

1.7.2 Carbonyl cyanide-p-trifluoromethoxyphenylhydrazone (FCCP)

FCCP is a weak, acidic, chemical compound known to induce uncoupling between the electron transport chain and the oxidative phosphorylation (the ATP synthase), by dissipating the proton gradient across the inner mitochondrial membrane. Its uncoupling properties are thought to be attributable to its protonophoric actions [51, 56-58].

The hydrophobicity and the electron-withdrawing ability are important factors of most weak, acidic uncouplers. The anionic part of the uncoupler, U^-, traps the H^+ ions, thus forming the neutral form UH (figure 1.8). UH traverses the mitochondrial inner membrane to the opposite side where it releases H^+, thus H^+ reenters the mitochondrial matrix, while U^- returns to the original interface where it traps a new H^+ ion. In this way, the H^+ gradient across the inner mitochondrial membrane is being dissipated, thus resulting in uncoupling[58].

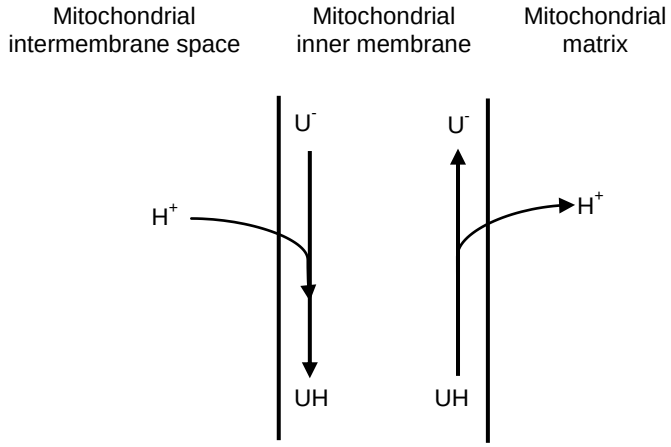

Figure 1.8: Simplified overview of the action of weak acidic uncoupler. Figure modified from Terada [58].

1.8 Aims/purposes of the study

This study was designed to determine whether there are physiological and biochemical differences between myoblasts and myotubes from type 2 diabetic vs. myoblasts and myotubes from non-diabetic subjects with regard to their:

1) Energy metabolism properties
2) Mitochondrial content and mass
3) OXPHOS content and ATP concentration
4) Differentiation capacity

The primary aim for this study was to determine the metabolic properties of myoblast and myotubes by measuring the rates of oxygen consumption (OCR) and extracellular acidification (ECAR). This was done under non-modulated (baseline) and modulated (with addition of oligomycin, which inhibits the ATP synthase, and carbonyl cyanide-p-trifluoromethoxy-phenylhydrazone (FCCP), which disrupts the membrane potential across the inner mitochondrial membrane) conditions. The OCR is an indicator of the mitochondrial respiration, while ECAR is an indicator of lactic acid production or glycolysis.

Whether there are differences (or not) in the metabolic properties of cells from these two donor groups led to possible hypothesis for explanation, and, therefore, secondary aims, namely:

- Determine the mitochondrial content and mass
- Determine OXPHOS content and ATP concentration
- Determine the protein content of a marker for differentiation capacity, myosin heavy chain (MHC)

2 Materials and methods

2.1 Materials

2.1.1 Cell culturing

Dulbecco's modified Eagle medium with GlutaMax (DMEM low glucose), fetal bovine serum (FBS), human epidermal growth factor (HuEGF), minimum essential media with GlutaMax (αMEM), Hank's balanced salt solution (HBSS) and 1X Dulbecco's phosphate buffered saline (DPBS) were obtained from Invitrogen, Carlsbad, CA 92008, USA. Bovine serum albumin (BSA), dexamethasone, and antibiotic/antimycotic stock solution (100X, 10.000 U penicillin, 10 mg streptomycin, 25 µg amphotericin B/ml) were obtained from Sigma, St. Louis, MO 63178, USA. Fetuin was obtained from Akron Biotech, Boca Raton, FL 33487, USA. Trypsin/EDTA was obtained from Lonza AG, 50829 Cologne, Germany. Cell culture dishes (6-well plates, 12-well plates and 96-well plates) and cell culture flasks (T75 flasks) were purchased from Corning, Corning, NY 14831, USA.

2.1.2 Measuring metabolic properties

XF assay medium, XF calibrant solution, XF24-well calibration plates, XF24 dual-analyte sensor cartridges and XF24-well cell culture microplates were obtained from Seahorse Bioscience, Chicopee, MA 01022, USA. D-(+)-glucose, oligomycin and carbonyl cyanide-p-trifluoromethoxyphenylhydroazone (FCCP) were obtained from Sigma, St. Louis, MO 63178, USA. OCR and ECAR were measured with the XF24 Analyzer from Seahorse Bioscience, Chicopee, MA 01022, USA.

2.1.3 Western immunoblotting

10X cell lysis buffer (CLB) was obtained from Cell Signaling Technology, Danvers, MA 01923, USA. Total protein content was measured with the SpectraMax Plus384 Absorbance Microplate Reader from Molecular Devices, Sunnyvale, CA 94089-1136, USA. Protease

inhibitor cocktail solution, Trizma® base, glycine, methanol and Tween 20 were obtained from Sigma, St.Louis, MO 63178, USA. Mini-PROTEAN®TGX™ Precast Gels (4-15 %), Immuno-Blot™ membrane for protein blotting (0.2 µm), 10X Tris/Glycine/SDS buffer, 10X tris buffered saline (TBS) and non-fat milk for blocking were obtained from BIO-RAD, Hercules, CA 94547, USA. 10X phosphate buffered saline (PBS) was obtained from Fisher Scientific, Pittsburg, PA 15275, USA. Nuclease free water was obtained from Ambion, Foster City, CA 94404, USA. ddH_2O was obtained from MilliQ QGARD®2 from Millipore, Billerica, Massachusetts 01821, USA. 927-4000 Odyssey® Blocking Buffer was obtained from LI-COR, Lincoln, Nebraska USA. The antibodies were obtained from Hybridoma Bank, Iowa City, Iowa 52242-1324, USA (MF20 mouse anti-human myosin), Abcam, Cambridge, MA 02139-1517, USA (mouse anti-human GAPDH antibody [mAbcam 9484]), Mitoscience, Eugene, Oregon 97403, USA (MitoProfile® Total OXPHOS Human WB Antibody Cocktail), Santa Cruz Biotechnology, Santa Cruz, CA. 95060, USA (Goat-anti-mouse IgG-HRP) and Invitrogen, Carlsbad, CA, USA (goat anti-mouse IgG Alexa Fluor 680). Lumigen™ PS-3 detection reagents were obtained from GE Healthcare. F-BX810 X-ray film was purchased from Phenix Research Products, Candler, NC 28715, USA. Bands for ECL Western Blots were visualized with Kodak K X-OMAT 1000A Processor (Rochester, NY, USA) and densitometry values were quantified by using Gel Pro Analyzer 3.1 (Bethesada, MD, USA). Bands for Odessey Western Blots were visualized and densitometry values were quantified by using an Odyssey 9120 Infrared Imaging System (LI-COR, Lincoln, NE).

2.1.4 Real time polymerase chain reaction (rt-PCR)

RNeasy® and DNeasy® kits were obtained from QIAGEN, Valencia, CA 91355, USA. 10X DNase I Reaction Buffer and DNase I Amp Grade 1 U/µl were obtained from Invitrogen, Carlsbad, CA 92008, USA. 5X iScript reaction mix and iScript reverse transcriptase were obtained from BIO-RAD, Hercules, CA 94547, USA. TaqMan 2X Universal PCR Master Mix was obtained from Applied Biosystems, Foster City, CA 94404, USA. PCR plates and 18S (Hs03928990_g1) were purchased from Applied Biosystems, Foster City, CA 94404, USA. ND1* and ND4* were in house reagents at PBRC. Robotic pipetting was done by MULTIPROBE II PLUS HT EX from PerkinElmer, Waltham, MA 02451, USA.

* See appendix for sequences

PCR reactions were carried out by ABI PRIS 7900 HT Fast Real Time PCR System, from Applied Biosystems, Foster City, CA 94404, USA.

2.1.5 Mitotracker measurements

MitoTracker® green was obtained from Invitrogen, Carlsbad, CA 92008, USA. Dimethyl sulfoxide (DMSO) was obtained from Sigma, St. Louis, MO 63178, USA. Mitochondrial content was measured with a luminometer, the Luminescence Spectrometer Model LS-50B, from PerkinElmer, Waltham, MA 02451, USA.

2.1.6 ATP measurements

The EnzyLight™ ATP Assay Kit was obtained from BioAssay Systems, Hayward, CA 94545, USA. Trichloroacetic acid (TCA) and xylenol blue were obtained from Sigma, St. Louis, MO 63178, USA. Total ATP content was measured with a luminometer, the Synergy 2 Multi-Mode Microplate Reader, from BioTek, Winooski, VT 05404, USA.

2.2 Study population

The experiments were conducted by using samples from type 2 diabetic (T2D) and non-diabetic (N-D) subjects from studies completed at The Pennington Biomedical Research Center. The studies included ACITIVE II, CALERIE, EAT, MARTI, MITO, TAKE TIME and USDA. The characteristics of the subjects are provided in table 2.1. All muscle biopsies used in this study were taken at baseline (pre-intervention), and all of the experiments were conducted by using immunopurified human skeletal muscle satellite cells, at passage four (p4). Passage is defined as a single expansion followed by subculturing. The satellite cells were immunopurified by using the mouse monoclonal 5.1H11 anti-CD56 antibody from Hybridoma Bank, Iowa City, Iowa 52242-1324, USA. Purified satellite cells proliferate robustly *in vitro* and respond to environmental cues to differentiate into mature myotubes[59].

Table 2.1: Characteristics of the study participants. All data are given as mean ± S.E.M and analyzed by using the Mann-Whitney test. Values with $*P < 0.05$, is considered significantly different from N-D subjects.

	Type 2 diabetic subjects (*n*=10)	Non-diabetic subjects (*n*=10)
Age (years)	53.2 ± 4.4*	28.7 ± 2.3
Height (cm)	167.8 ± 3.2	172.0 ± 1.6
Weight (kg)	101.7 ± 5.1*	74.2 ± 2.7
BMI (kg/m^2)	36.0 ± 1.3*	25.0 ± 0.6
Body fat (%)	37.2 ± 2.1*	23.2 ± 2.0
Race (black/white)	3/7	1/9
Sex (male/female)	7/3	7/3

2.3 Cell culturing

2.3.1 Myotube differentiation

After sorting, cells were cryopreserved in 10 % DMSO and stored in liquid nitrogen until the experiments. Cryopreserved sorted human muscle satellite cells (myoblasts) were quickly thawed in water bath at 37 °C. The content of the cryovial (1 ml) was resuspended in 3 ml growth medium*, and mixed well by pipetting. The solution was then divided into four T75

* See appendix

flasks with 25 ml growth medium. The flasks were incubated at 37 °C/5 % CO_2 overnight to allow for attachment. The growth medium was changed the following day to get rid of toxic DMSO. Medium change was scheduled every other day until ~80 % cell confluence was reached.

After reaching ~80 % confluence, cells were harvested by removing the media and washing the T75 flask with 10 ml HBSS or DPBS. The cells were removed from the flasks by the addition of 3 ml Trypsin/EDTA to each flask followed by incubation at 37 °C/5 % CO_2 for 3-5 minutes. The trypsin/EDTA solution was neutralized by the addition of growth medium followed by gentle pipetting. Centrifugation at 2000 RPM for 5 minutes and re-suspension of the resulting cell pellets in growth medium for counting. At ~80 % confluence, myotube differentiation was achieved by removing the growth medium, and changing to differentiation medium* for a period of 5-7 days.

Seeding in XF24-well cell culture micro plates

The XF24 Analyzer protocol (Seahorse Bioscience) was used for seeding in the XF24-well cell culture microplates. Briefly, cells were counted using a hemocytometer and resuspended at a density of 3.0 x 10^5 cells/ml in growth medium. Cultures were seeded in XF24-well cell culture microplates at 3.0 x 10^4 cells/well in 100 µl growth medium, and incubated at 37 °C/5 % CO_2 for 1 hour. After cell attachment, an additional 150 µl growth medium was added and cultures were incubated at 37 °C/5 % CO_2 for 24 – 48 hours. The cells were seeded as shown in 2.1.

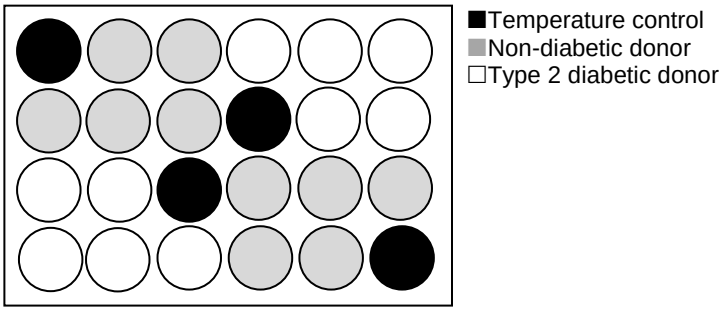

Figure 2.1: Schematic of seeding on XF24-well cell culture microplates. Seeding was designed to minimize variability associated to well position. The open wells are for temperature control during experiments in the XF24 Analyzer.

* See appendix

Seeding in 96-well plates for determination of ATP concentration and mitochondrial mass

Cells were counted using a hemocytometer and adjusted to a final concentration of 3.0 x 10^5 cells/ml in growth medium. The cells were then seeded in 96-well plates at 3.0 x 10^4 cells/well in 100 µl growth medium, following incubation at 37 °C/5 % CO_2 for 1 hour, to allow for attachment. After cell attachment, an additional 150 µl growth medium was added and cultures were incubated at 37°C/5 % CO_2 for 24 hours prior to differentiation.

Seeding in 12-well plates for DNA, protein, RNA and ATP extraction

Cells were counted using a hemocytometer and adjusted to a final concentration of 2.5 x 10^5 cells/ml in growth medium. 1 ml of cell suspension was added to each well and briefly pipetted up and down to insure even distribution. Medium change was scheduled every other day until ~80 % confluence. The cultures were differentiated by the addition of differentiation medium which was changed every 2 days during the experiment. DNA, protein, RNA and ATP were extracted pre- (day 0) and post-differentiation (day 5) following storing at -80 °C until further analysis.

2.4 Measuring metabolic properties

To assess the metabolic properties of T2D and N-D subjects, experiments were carried out in real time, on live cells, in the XF24 Analyzer. This is a non-invasive method that can measure physiological changes in cellular energetic and metabolic pathways *in vitro*. The XF24 Analyzer measures the shift between aerobic respiration and glycolysis in the cells (i.e. rates of oxygen consumption and extracellular acidification, respectively).

2.4.1 The XF24 extracellular flux analyzer

The principle of measurements in the XF24 Analyzer is illustrated in figure 2.2. The XF24 Analyzer uses fluorescent sensors to measure extracellular fluxes of oxygen consumption (OCR) and extracellular acid release (ECAR) from the cells. The fluorescent sensors are placed on a plastic biocartridge which is placed on top of the cell culture microplate.

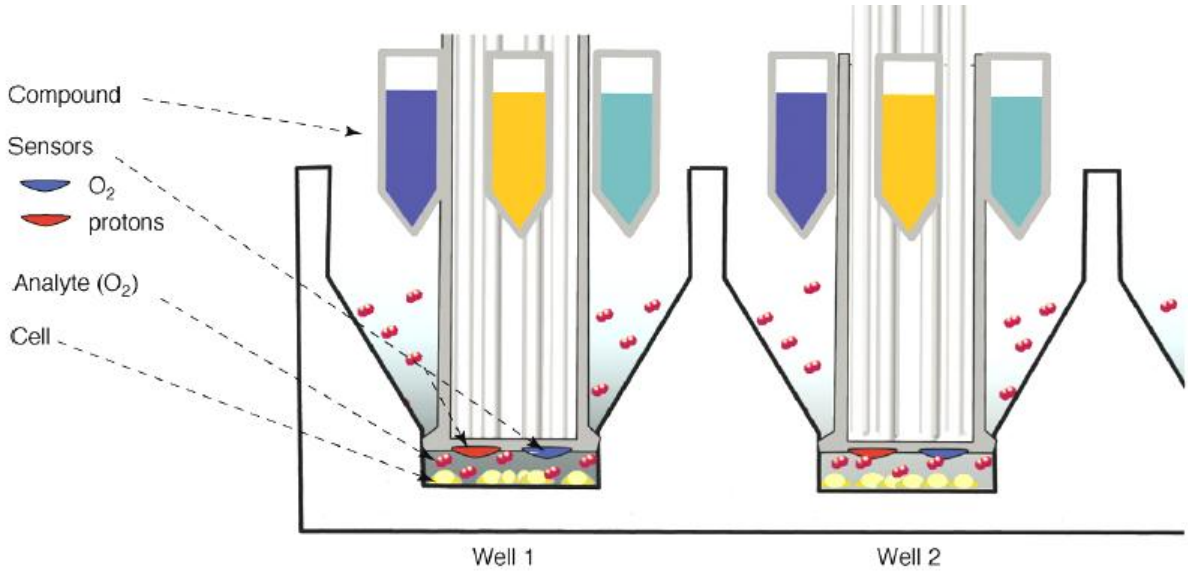

Figure 2.2: Measuring bioenergetics of skeletal muscle cells by using the XF24 extracellular flux analyzer. The figure shows a cutaway view of the XF24 cell culture microplate and sensor biocartridge. Figure from Ferrick et al.[60]

By lowering the biocartridge to approximately 200 µm above the cells, a temporary 7 µl micro chamber, with limited diffusion, is being formed. This helps speeding up the measurements. Over a time period of 1.5 – 4 minutes, the depletion of oxygen or decrease in pH is being measured, before the fluorescent sensors return to their original position. During this time period, the medium is re-equilibrated, before the sensors are lowered again and ready for new measurements. The sensor plate has four injection sites per cell well, which makes it possible for multiple injections of different reagents in a single experiment[60].

OCR and ECAR were measured by following the XF24 Analyzer protocol (Seahorse Bioscience) as previously described by Wu et al.[61], with some modifications. OCR and ECAR measurements were obtained pre- (day 0) and post-differentiation (day 5) for myoblasts and myotubes, respectively. Growth medium/differentiation medium was removed from each well and replaced with 625 µl of pre-warmed (37 °C) assay medium (unbuffered DMEM with 5 mM glucose at pH 7.4), following 1 hour incubation at 37 °C, to allow the medium temperature and pH to reach equilibrium. The XF24 Analyzer measured OCR and ECAR simultaneously for baseline and after the addition of oligomycin and FCCP.

To allow the oxygen partial pressure to reach equilibrium before each rate measurement, the XF24 analyzer gently mixed the assay media in each well for 8 minutes. To establish baseline rate, the OCR and ECAR were measured simultaneously for 3 minutes followed by oligomycin (75 µl 50 µM, final concentration in the wells; 5.4 µM*) and FCCP (75 µl 10 µM, final concentration in the wells; 1.0 µM*) injections with subsequent rate measurements. There were 3 baseline-, 3 oligomycin- and 3 FCCP- response rates measured, with 3-5 minutes of mixing between each measurement to restore normal oxygen tension and pH. After the assay, DNA and protein were extracted from the plates and samples stored at -80 °C until further analysis.

2.5 Extraction of DNA, protein and ATP for quantification

2.5.1 DNA

Total DNA was extracted from the cells by using the DNeasy® Blood & Tissue Kit (QIAGEN). Briefly, the cells were lysed in the wells; and ethanol was added to each well. The cell suspension was then transferred to a centrifugal tube, where the DNA selectively binds to the DNeasy column. The column was then washed twice to remove contaminants and enzyme inhibitors. Extracts were collected in a final volume of 100 µl of elution buffer. DNA samples were quantified by using a spectrophotometer, ND-100 from NanoDrop®, following storing at -80 °C until further analysis.

* See appendix for calculations

2.5.2 Protein

Total protein was extracted from the cells by adding cell lysis buffer (CLB) to each well (15µl and 150 µl for XF24 cell culture microplates and 12-well plates, respectively). The cell suspension was transferred to an Eppendorf tube and protein levels were quantified by using the Bio-Rad Protein Assay as previously described by Bradford et al[62]. Briefly, 10 µl of protein standards (made from BSA and diluted to known concentrations), as well as homogenized cell lysate from each sample was transferred to a 96-well plate. 200 µl bicinchoninic acid (BCA) protein assay reagent (with a 1:5 dilution of reagent A and B respectively), was then added to all the wells with standards and samples, following incubation at 37 °C for 30 minutes. $Absorbance_{(565)}$ values were determined by using the SpectraMax Plus384 Absorbance Microplate Reader.

Protein samples with concentration levels lower than 1 mg/ml were concentrated using Amicon® Ultra-0.5 protocol from Millipore. The protein samples were pipetted into the Amicon Ultra filter devices and centrifuged at 14.000 RCF for approximately 1-10 minutes, depending on the desired end volume. The Amicon Ultra filter devices were then placed upside down into clean micro centrifuge tubes, and spun for 2 minutes at 1000 RCF to transfer the concentrated samples from the filter devices to the tubes. Protein levels were re-quantified by using the Bio-Rad Protein Assay (as described above). Protein samples were stored at -80 °C until further analysis.

2.5.3 ATP

ATP from cell lysate

Total ATP was extracted from the cells by adding 150 µl 5 % trichloroacetic acid (TCA) to each well. The cell suspension was transferred to an Eppendorf tube, and the cells were homogenized with a plastic homogenizer and then spun down at 2000 RPM for 2 minutes at 4 °C. The supernatant was stored at -80°C until further analysis.

ATP samples were neutralized to pH 7.4 as described by Luo and Luo[63]. Briefly, 50 µl of each ATP sample (in 5 % TCA) was neutralized to pH 7.4 by adding 4 µl saturated tris base, 450 µl ddH_2O and 5 µl 2 % xylenol blue for pH control. Xylenol blue is a pH indicator

which is red in TCA (indicating pH <1.2) and yellow at pH 7.4 [64]. The final pH was measured by pH indicator strips to ensure neutral pH.

The ATP concentration was assessed quantitatively by using the EnzyLight™ ATP Assay Kit, as previously described[65]. Briefly, 100 µl of each ATP standard (made from 3mM ATP standard and diluted to known concentrations), and homogenized ATP samples were transferred into wells of a white opaque 96-well plate. 90 µl of Reconstitued Reagent (95 µl Assay Buffer, 1 µl Substrate and 1µl ATP Enzyme), was then added to all the wells with standards and samples, following incubation at room temperature for 10 minutes. Light photons were measured by a luminometer (Synergy 2 Multi-Mode Microplate Reader, BioTek), and compared with an ATP standard curve (concentrations from 0-12 µM ATP) to calculate ATP concentration (µM).

ATP live cells

ATP concentration was measured in live cells post-differentiation (day 5). The differentiation medium was removed from the wells, and each well was rinsed with DPBS (twice). ATP concentration was measured by using the EnzyLight™ ATP Assay Kit (BioAssay Systems) as described above.

2.6 Western immunoblotting

2.6.1 Determination of MHC content (ECL Western immunoblotting)

Protein samples were either diluted (with RIPA buffer, proteinase and phosphotase inhibitors) or pooled, to get a final concentration of 1 µg/µl per sample, with an end volume of 50 µl. Denaturation agent with dye (bromophenol blue, SDS, mercaptoethanol, tris base) was added to each sample and the sample was heated to 95 °C for 2 minutes. Western immunoblotting was performed as described by Lou and Lou[63]. Briefly, 25 µg protein of each sample was loaded on to Mini-PROTEAN®TGX™ Precast Gels (4-15 %). After electrophoresis (150V, room temperature, for approximately 1 hour), the proteins were

transferred onto the membranes (Immuno-Blot^{TM} Membrane for protein blotting, 0.2 μm) for 1 hour (100V, 4 °C) in a transfer buffer*. The membranes were then washed for 5 minutes with washing buffer* (this was repeated three times) and blocked for 1 hour with blocking buffer* (both at room temperature). MF20 mouse anti-myosin (1:500, Hybridoma bank) was used for MHC expression, and mouse anti-GAPDH (1:100, Abcam) was used as loading control. Membranes were incubated with primary antibodies over night at 4 °C, and then probed with IgG-HRP goat anti-mouse (1: 10 000, Santa Cruz Biotechnology) as a secondary antibody for 1 hour at room temperature. Bands were visualized by using Amersham ECL Plus Western Blotting Detection Reagents protocol (GE Healthcare). Briefly, excess wash buffer was drained from the membranes. They were placed protein side up on a plastic folder, and detection solution was added following incubation for 2 minutes at room temperature. Excess detection solution was drained from the membranes and the immunoblots were developed. Densitometry value was quantified by using Gel Pro Analyzer 3.1.

2.6.2 Determination of OXPHOS content (Odyssey Western immunoblotting)

Protein samples were prepared and transferred to membranes (Immuno-Blot^{TM} Membrane for protein blotting, 0.2 μm) as described above.

OXPHOS (1:500, MS601; MitoSciences, Eugene, OR), a primary antibody cocktail was used for Complex I,II,III,IV&V expression at the same time, and GAPDH (1:1000, ab9484, Abcam, Cambridge, MA) was used as loading control. Membranes were incubated with primary antibodies overnight at 4 °C, and then probed with goat anti-mouse IgG Alexa Fluor 680 (1:10.000, Invitrogen, Carlsbad, CA) as a secondary antibody for 1.5 hours at room temperature. Bands were visualized and densitometry value was quantified by using an Odyssey 9120 Infrared Imaging System (LI-COR, Lincoln, NE).

* See appendix

2.7 Real Time Polymerase Chain Reaction (rt-PCR)

Mitochondrial content was measured by the number of copies of mitochondrially encoded NADH dehydrogenase subunit 1 and 4 genes (ND1 and ND4, respectively). DNA samples were diluted with nuclease free water to a concentration of 1.66 ng/µl. 50 µl of each sample, as well as standards, master mix, primers and probes were added to a 96-well plate. Robotic pipetting to PCR plates was done by MULTIPROBE II PLUS HT EX from PerkinElmer. Rt-PCR reactions were carried out by ABI PRIS 7900 HT Fast Real Time PCR System, from Applied Biosystems.

2.8 Mitotracker

Mitochondrial mass was measured by using the MitoTracker® Mitochondrion-Selective Probes Assay from Invitrogen. The assay was performed on differentiated live myotubes (day 5) directly in the 96 well plate. The differentiation media was removed from the wells, and each well was rinsed with DPBS (twice). 100 µl of mitotracker solution C (see appendix) was added to each well, following incubation at 37 °C for 30 minutes. Mitotracker solution C was removed from the wells, and each well was rinsed with DPBS (twice) before adding 200 µl PBS to each well. Fluorescent intensity was determined with the Luminescence Spectrometer Model LS-50B (excitation and emission wavelength of 450 nm and 516 nm).

2.9 Statistical analysis

All data are reported as means ± S.E.M. The comparison of differences between type 2 diabetic and non-diabetic cells were analyzed with SigmaStat® version 3.11 (Statistical Analyzing Software, Richmond, CA, USA), and evaluated by the Mann-Whitney test (also termed the Wilcoxon rank sum test). $P < 0.05$ was considered statistically significant, and statistical significant observations are marked with *.

3 Results

The characteristics of the study population are presented in table 2.1. In general, subjects were young to middle-aged men and women with a broad range of BMI (21.2 – 44.5 kg/m^2) and fatness (14.0 – 51.2 %). The study included 10 subjects with type 2 diabetes (T2D) and 10 subjects with no history of diabetes (N-D). All experiments were conducted on muscle cells established at baseline (pre-intervention).

Assessment of metabolic properties was conducted on 5 donor pairs, i.e. 5 T2D and 5 N-D donors, and not the whole study population, due to time limitation. Determination of mitochondrial content and mass, in addition to ATP concentration were also conducted on 5 donor pairs. Assessment of OXPHOS and MHC content were supposedly conducted on 10 donor pairs, but due to insufficient amount of protein from one donor pair, the experiments were only conducted on 9 of the 10 donor pairs.

3.1 Metabolic properties of skeletal muscle cells from type 2 diabetic and non-diabetic subjects

The purpose of these experiments was to assess the metabolic properties of skeletal muscle from T2D and N-D donors, and determine possible differences between the two groups. This was achieved by performing real time measurements of mitochondrial respiration (oxygen consumption rate, OCR) and glycolysis (extracellular acidification rate, ECAR) at baseline and with the addition of oligomycin and FCCP. Measures of respiration were normalized to DNA content, rather than protein content, due to insufficient protein extractions from the XF24-well cell culture microplates. Normalizing to protein values would thus give incorrect results. Both DNA-normalized and non-normalized data (not shown) gave similar results.

Myoblasts were grown in T75 flasks until they reached ~80 % confluence. They were then harvested and re-seeded in the XF24-well cell culture microplates (100 µl per well, with concentration 3.0 x 10^5 cells/ml, i.e. 3.0 x 10^4 cells/well). Assays were performed pre-differentiation and 5 days post-differentiation on myoblasts and myotubes, respectively.

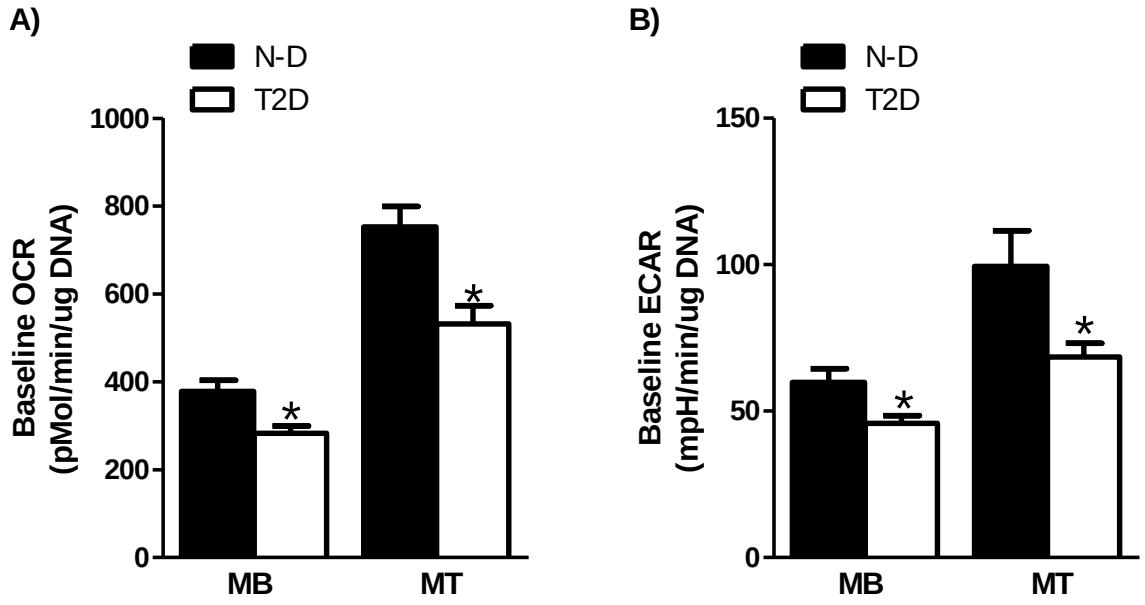

Figure 3.1: Mitochondrial respiration rate (OCR) and glycolysis rate (ECAR) of human skeletal muscle cells. Myoblasts (MB) and differentiated myotubes (MT) were established from 5 obese type 2 diabetic (T2D) subjects and 5 lean, healthy control subjects (N-D). **A)** Basal cellular respiration rate (OCR) of the two donor groups. **B)** Basal extracellular acidification rate (ECAR) of the two donor groups. All data are given as mean ± S.E.M., and the Mann-Whitney test was applied for comparison of the two donor groups. Both rates were normalized to DNA content and expressed as rate per µg DNA. * $P<0.05$ vs. N-D cells.

Not surprisingly, assessment of metabolic properties under non-modulated conditions (baseline) showed significantly lower OCR and ECAR in T2D cells compared with cells from the control group (figure 3.1). The results showed that the T2D group had almost 30 % lower OCR, and 20-30 % lower ECAR, compared with the control group.

Oligomycin inhibits the mitochondrial respiration by blocking the ATP synthase. Injecting oligomycin to the media surrounding the cells will cause a drop in OCR. Since the cells are unable to synthesize ATP via oxidative phosphorylation, they revert to glycolysis to meet their demand for ATP. We therefore expect to see a change in pH as a result of lactate and H^+ production (acidification).

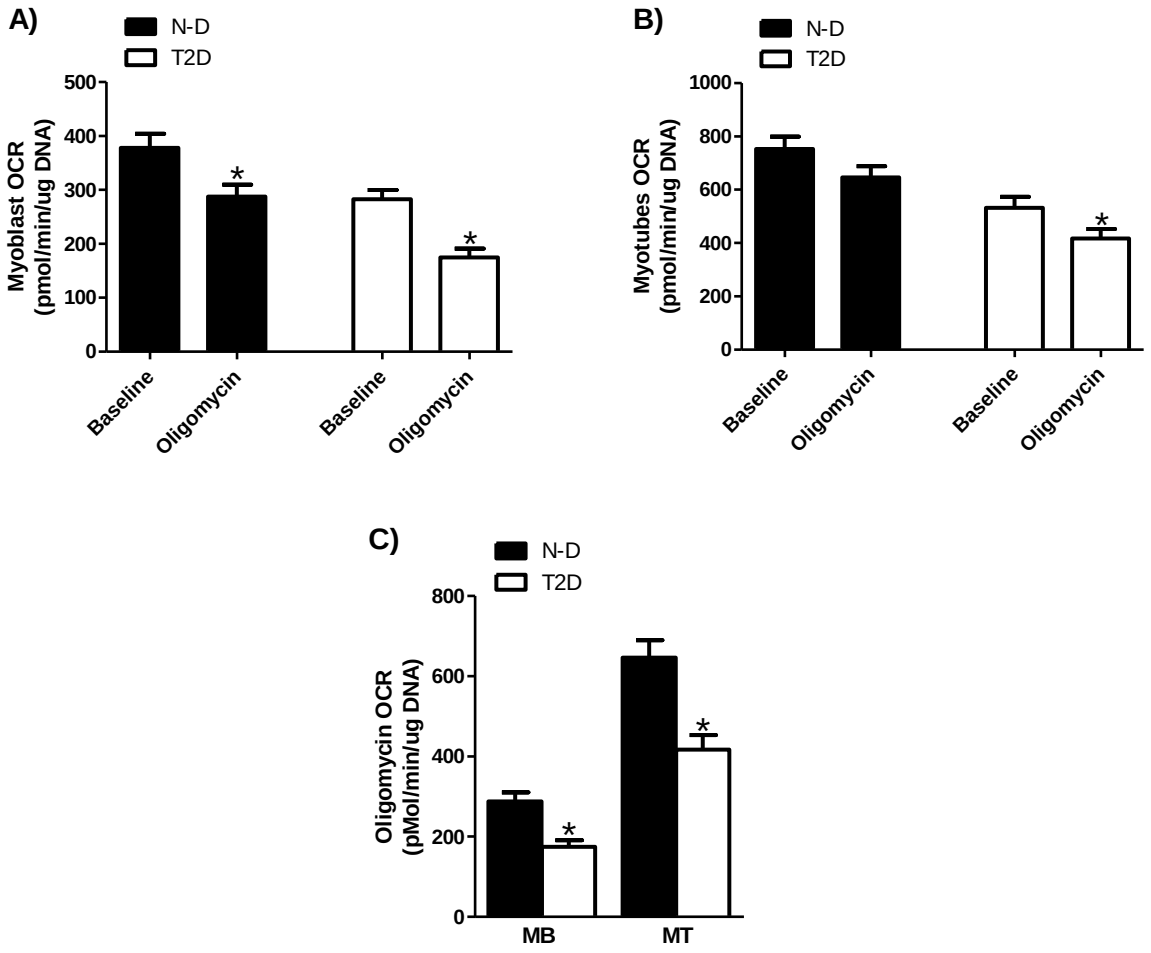

Figure 3.2: Oligomycin-modulated mitochondrial respiration rate (OCR) of human skeletal muscle cells. Respiration measured at baseline and in response to oligomycin (75 µl 50 µM) for **A)** myoblasts (MB) and **B)** myotubes (MT) from the two donor groups. **C)** Oligomycin (75 µl 50 µM) modulated cellular respiration (OCR) of the two donor groups. All data are given as mean ± S.E.M, and the Mann-Whitney test was applied for comparison. Both rates were normalized to DNA content and expressed as rate per µg DNA. **P*<0.05 vs. baseline measurements(**A**&**B)** and N-D cells(**C**).

Injections of oligomycin (5.4 μM, final concentration in each well) led to a significant drop in OCR compared to baseline measurements, as expected (except for N-D myotubes, P = 0.07) (figure 3.2 A & B). Cells from T2D subjects had significantly lower oligomycin OCR and ECAR compared to the control group (figure 3.2 C & 3.3 A), which may be due to a lower starting point at baseline (see figure 3.1).

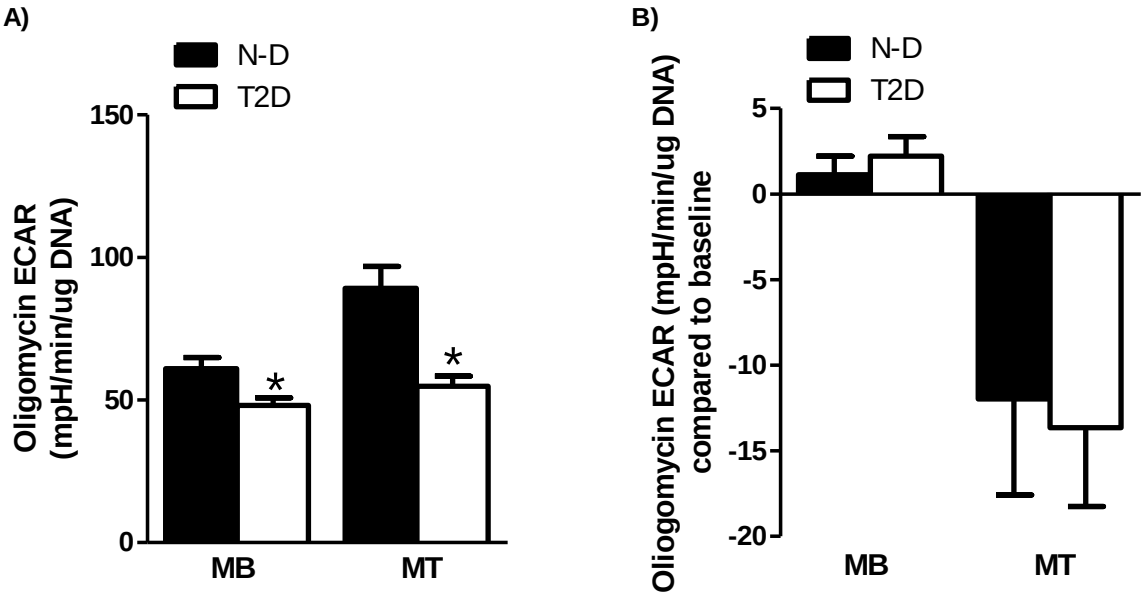

Figure 3.3: Oligomycin-modulated glycolysis rate (ECAR) of human skeletal muscle cells. Glycolysis measured in response to oligomycin (75 μl 50 μM) in myoblasts (MB) and myotubes (MT). Oligomycin modulated **A)** extracellular acidification rate (ECAR), **B)** oligomycin ECAR compared to baseline ECAR measurements for the two donor groups. All data are given as mean ± S.E.M, and the Mann-Whitney test was applied for comparison of the two donor groups. Both rates were normalized to DNA content and expressed as rate per μg DNA. *P<0.05 vs. N-D cells.

The myoblasts did not show any significant change in pH, while the myotubes showed a negative pH change compared to baseline measurements (figure 3.3 B), indicating a switch from aerobic respiration to glycolysis.

FCCP acts as an uncoupler of oxidative phosphorylation within the mitochondria. This chemical compound disrupts the proton gradient over the inner mitochondrial membrane thus allowing for the protons to leak back to the mitochondrial matrix. Due to this disruption of membrane potential, the electron transport chain (ETC) tries to compensate by pumping as much protons into the intermembrane space as possible, thus leading to maximal oxygen consumption.

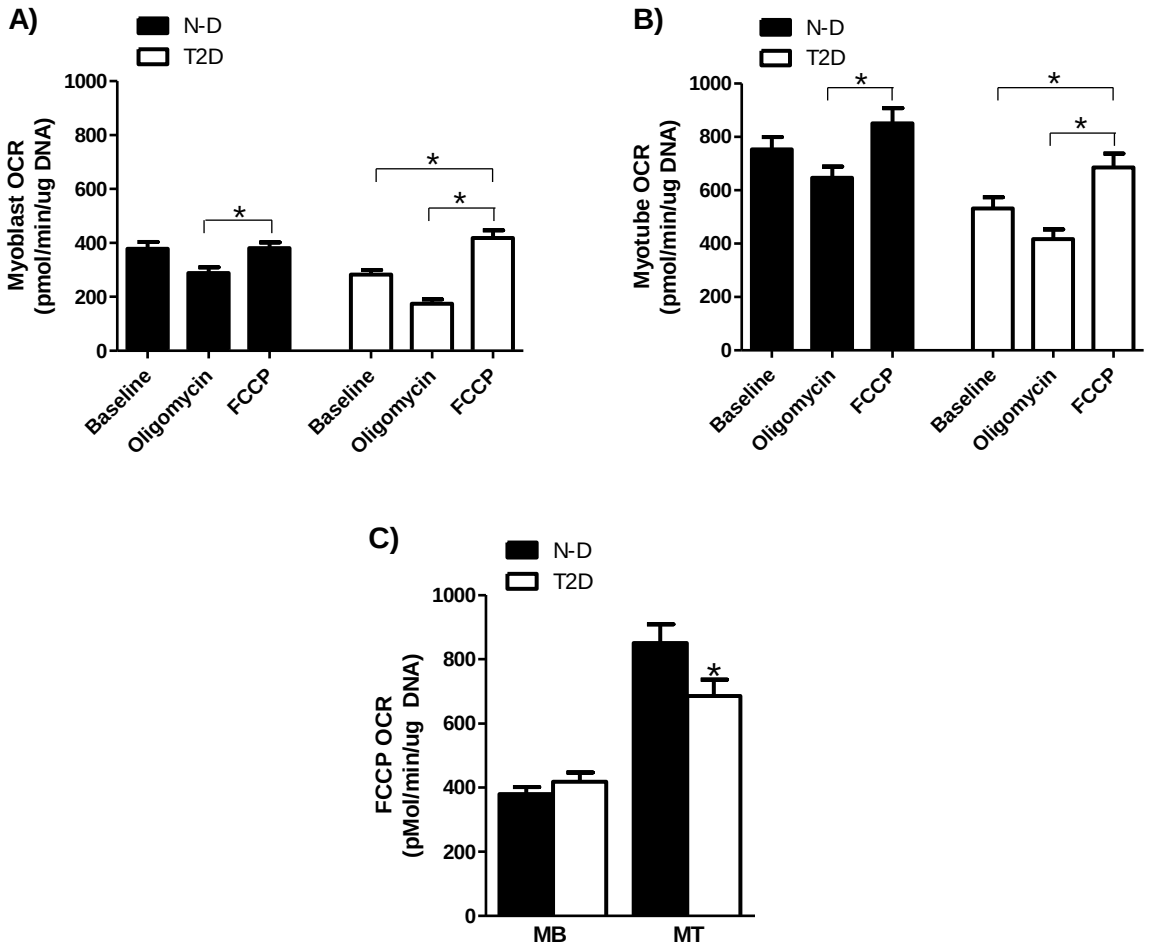

Figure 3.4: FCCP-modulated mitochondrial respiration rate (OCR) of human skeletal muscle cells. Respiration measured at baseline and in response to oligomycin (75 µl 50 µM) and FCCP (75 µl 10 µM) for **A)** myoblasts (MB) and **B)** myotubes (MT) for the two donor groups. **C)** FCCP (75 µl 10 µM) modulated cellular respiration (OCR) of the two donor groups. All data are given as mean ± S.E.M, and the Mann-Whitney test was applied for comparison. Both rates were normalized to DNA content and expressed as rate per µg DNA. **P*<0.05 vs. baseline and oligomycin measurements(**A**&**B)**, and N-D cells(**C**).

Injections of FCCP (1.0 µM, final concentration in each well) increased the OCR as a result of maximal O_2 consumption due to disruption of the proton gradient (figure 3.4 A & B). There was a significant increase in OCR from oligomycin measurements in both groups. There was also a significant increase in OCR compared to baseline measurements for T2D cells; this was not seen in cells from the control group (N-D) (figure 3.4 A & B). This may be due to a higher baseline OCR in the control group (see figure 3.1 A), i.e. these cells utilize a greater proportion of the maximal O_2 consumption at baseline.

Myoblasts did not show any significant difference in OCR between the two donor groups, while T2D myotubes had significantly lower OCR compared to the control group (figure 3.4 C), indicating a lower potential for maximal O_2 consumption in T2D cells.

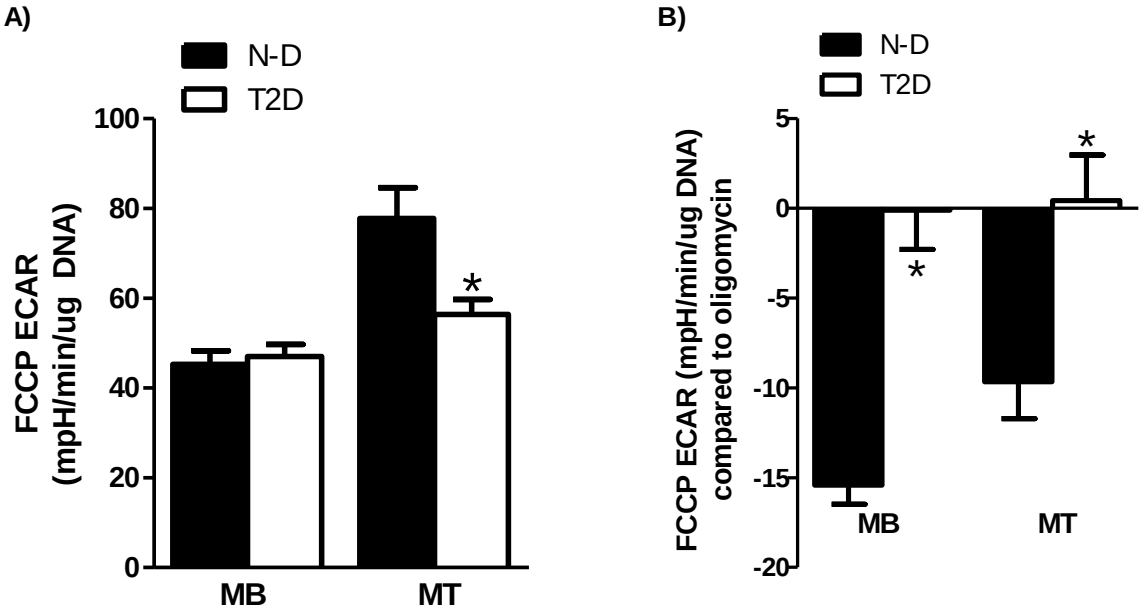

Figure 3.5: FCCP-modulated glycolysis rate (ECAR) of human skeletal muscle cells. Glycolysis measured in response to FCCP (75 µl 10 µM). FCCP modulated **A)** extracellular acidification rate (ECAR), **B)** FCCP ECAR compared to oligomycin ECAR measurements for the two donor groups. All data are given as mean ± S.E.M, and the Mann-Whitney test was applied for comparison of the two donor groups. Both rates were normalized to DNA content and expressed as rate per µg DNA. **P*<0.05 vs. N-D cells.

T2D myoblasts did not differ from N-D myoblasts, while T2D myotubes had significantly lower ECAR compared to N-D myotubes (figure 3.5 A). Compared to oligomycin measures, both myoblasts and myotubes in the control group had a negative pH change, while the T2D cells did not show a change in pH (figure 3.5 B).

3.2 Mitochondrial measurements

Assessment of mitochondrial respiration and glycolysis in cells from T2D and N-D subjects gave an indicator of the mitochondrial function in the two donor groups, indicating and impaired mitochondrial function in T2D cells compared to cells from the control group. Several studies have also shown a lower mitochondrial number in T2D subjects. To test the hypothesis of whether impaired mitochondrial function is due to lower cellular mitochondrial content we conducted experiments to determine the mitochondrial content and mass, OXPHOS content and the ATP concentration in the cells.

3.2.1 Determination of mitochondrial content

ND1 and ND4 are genes encoded by the mitochondrial DNA (mtDNA). By carrying out real time PCR on these genes, it is possible to measure the number of copies of mtDNA, which is an indirect measurement of mitochondrial content.

DNA was isolated pre-differentiation (day 0) and post-differentiation (day 5), for myoblasts and myotubes, respectively. There were no significant differences between groups for either one of the mitochondrial genes (ND1 and ND4) (figure 3.6). This implies that there was no difference in the amount of mitochondria between T2D and the control group.

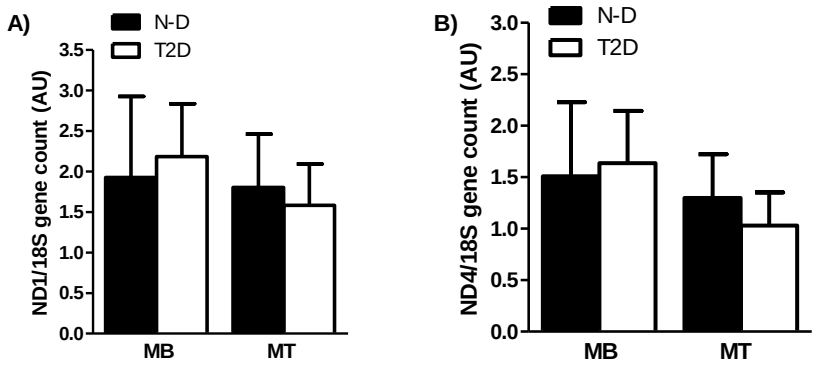

Figure 3.6: ND1 and ND4 gene count in human skeletal muscle cells. Myoblasts (MB) and differentiated myotubes (MT) were established from 5 obese type 2 diabetic (T2D) subjects and 5 lean, healthy control subjects (N-D). **A)** ND1 gene count and **B)** ND4 gene count. The figures show the relative values corrected for housekeeping gene 18S. Data was analyzed by ΔΔct. All data are given as mean ± S.E.M, and the Mann-Whitney test was applied for comparison of the two donor groups.

3.2.2 Determination of mitochondrial mass

The Mitotracker assay uses fluorescence to determine the mitochondrial mass. Regardless of the mitochondrial membrane potential, the Mitotracker Green Probe accumulates within the mitochondria, thus giving an estimate of the mitochondrial mass.

Myoblasts were grown in T75 flasks until they reached ~80 % confluence. They were then harvested and re-seeded in 96-well plates (100 µl per well, with concentration 3.0 x 10^5 cells/ml, i.e. 3.0 x 10^4 cells/well), following differentiation, 24-48 hours after plating. The mitochondrial mass was determined 5 days after induction of differentiation, by incubating cells with Mitotracker green. There were no significant differences between myotubes from the two donor groups (figure 3.7).

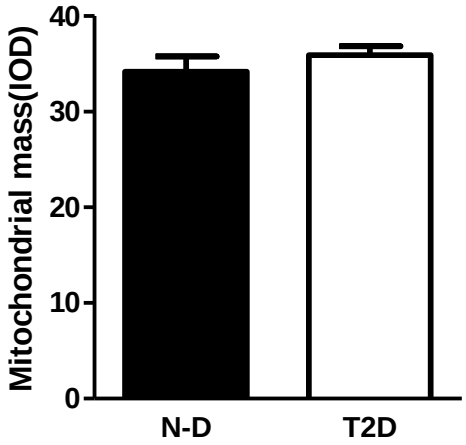

Figure 3.7: Mitochondrial mass measured in myotubes from type 2 diabetic and non-diabetic subjects. Myotubes were established from 5 obese type 2 diabetic (T2D) subjects and 5 lean, healthy control subjects (N-D). Mitochondrial mass was determined by measuring luminescence (at excitation and emission wavelength 490 nm and 516 nm). Data are given as mean ± S.E.M, and the Mann-Whitney test was applied for comparison of the two donor groups.

3.2.4 Determination of OXPHOS content

The OXPHOS Western immunoblotting kit, which contains a cocktail of monoclonal antibodies, was used to examine the relative levels of several subunits of the oxidative phosphorylation complexes. Complex I-IV contributes to the electron transport chain (ETC), while complex V synthesizes ATP from ADP (known as the ATP synthase), within the mitochondria. Subunits of the oxidative phosphorylation were examined to determine possible differences between myotubes from T2D and N-D subjects.

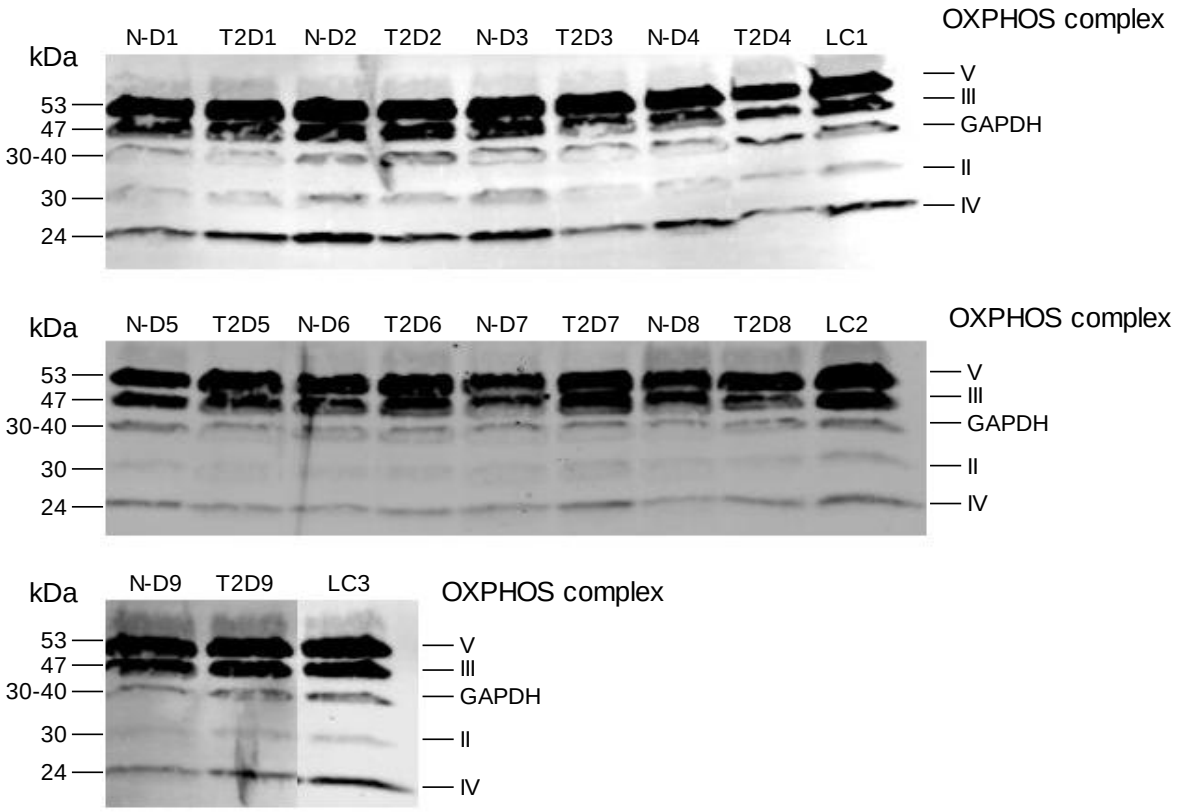

Figure 3.8: Expression of mitochondrial OXPHOS complexes in human myotubes. Differentiated myotubes were established from 9 obese type 2 diabetic (T2D) subjects and 9 lean, healthy control subjects (N-D). Loaded 25 µg of protein for each sample. Primary antibodies: MS601OXPHOS antibody cocktail for Complex I-V from MitoSciences at 1:500, 4 °C over night. Abcam ab9484 GAPDH antibody at 1:1000, 4 °C over night. Secondary antibody: IgG Alexa Fluor 680 from Invitrogen at 1:10,000. Bands were visualized and densitometry value was quantified by using Odyssey 9120 Infrared Imaging System. LC; loading control, GAPDH; Glyceraldehyde 3-phosphate dehydrogenase, OXPHOS; oxidative phosphorylation.

Experiments were conducted on myotubes 5 days after induction of differentiation. OXPHOS immunoblots are shown above (figure 3.8). There were no significant differences between myotubes from the two donor groups after quantification of the immunoblots (figure 3.9). The content of the OXPHOS complexes were not correlated to mitochondrial mass or mitochondrial content (data not shown).

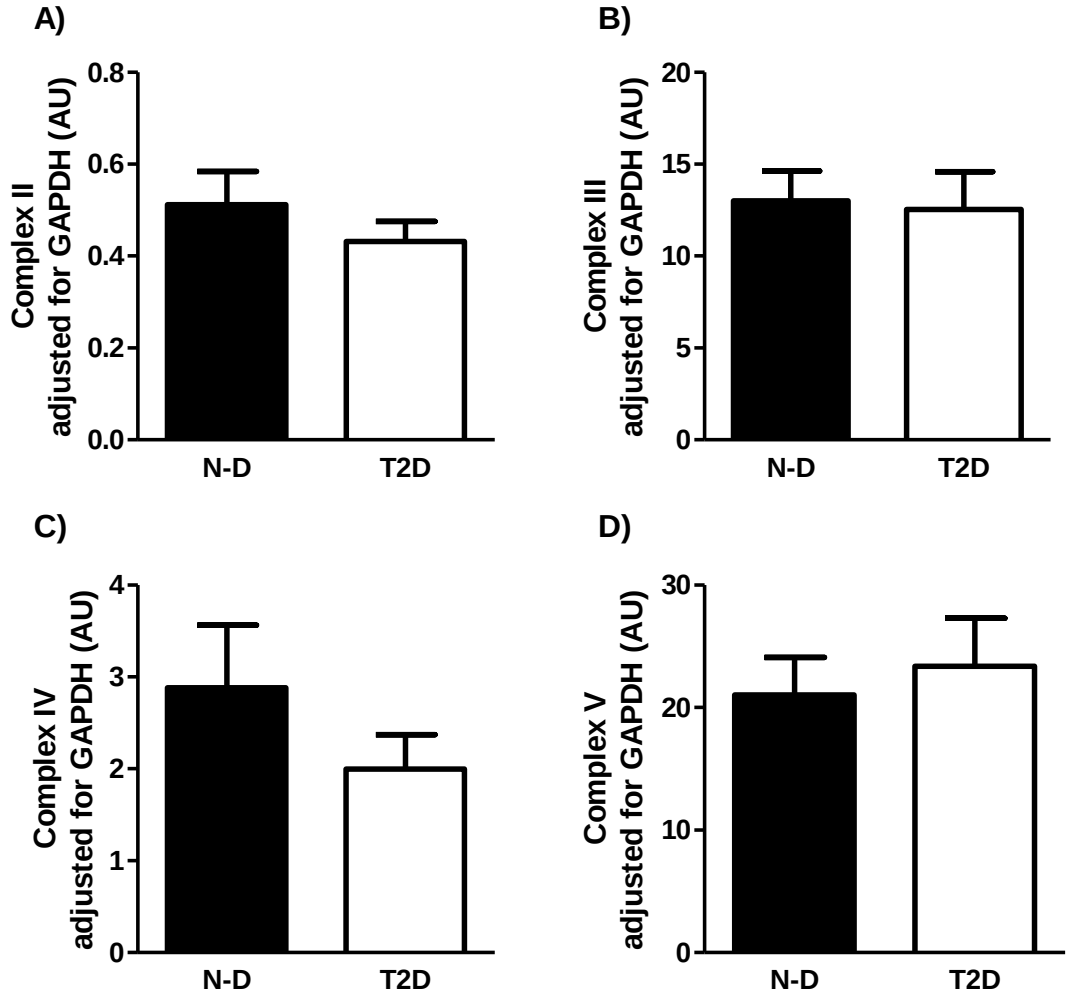

Figure 3.9: Content of mitochondrial OXPHOS complexes in human myotubes. Optical density plot showing the protein content of **A)** complex II, **B)** complex III, **C)** complex IV and **D)** complex V. All data are given as mean ± S.E.M, and the Mann-Whitney test was applied for comparison of the two donor groups. Values were normalized to GAPDH.

3.2.5 Determination of ATP concentration

The ATP concentration was assessed quantitatively by using the EnzyLight ATP Assay kit (BioAssay Systems). Experiments were conducted on cell lysate (myoblasts and myotubes) and live cells (myotubes).

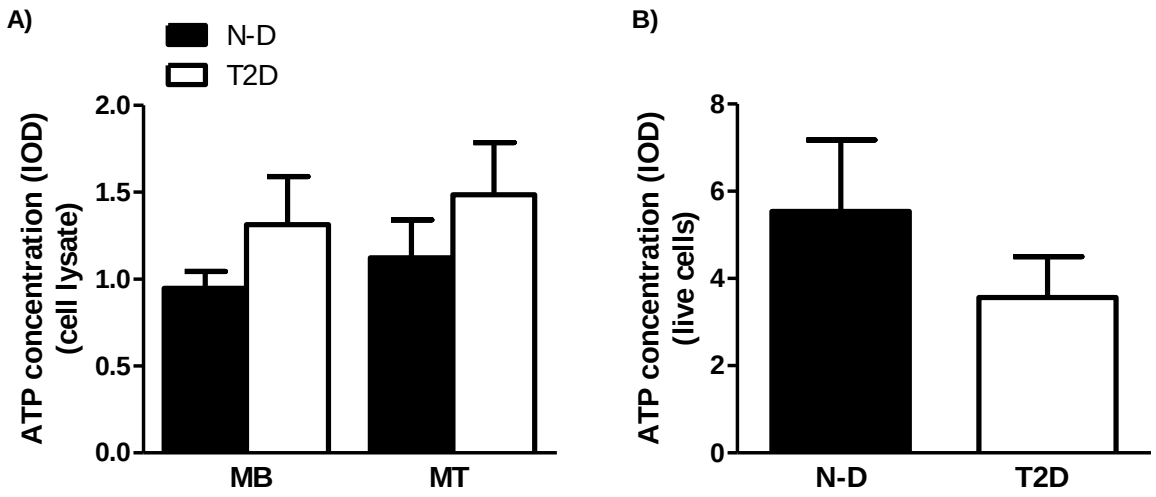

Figure 3.10: ATP concentration in human skeletal muscle cells. Myoblasts and differentiated myotubes were established from 5 obese type 2 diabetic (T2D) subjects and 5 lean, healthy control subjects (N-D). Light photons were measured by a luminometer (Synergy 2 Multi-Mode Microplate Reader, BioTek), and compared with an ATP standard curve to calculate ATP concentration. **A)** ATP concentration in cell lysate for myoblasts (day 0, pre-differentiation) and myotubes (day 5, post-differentiation) and **B)** ATP concentration in live cells for myotubes (day 5, post-differentiation). All data are given as mean ± S.E.M, and the Mann-Whitney test was applied for comparison of the two donor groups.

The results did not show any significant difference in ATP concentration between the two donor groups (figure 3.10).

3.3 Determination of myosin heavy chain (MHC) content

To get an indicator of the differentiation capacity, or the degree of differentiation, in our preparations of myotubes from T2D and N-D subjects, total protein was extracted from the cells, and 25 µg of each sample was run on a Western immunoblot. Myosin heavy chain (all MHCs expressed in human skeletal muscle cells) was used as a marker for differentiation capacity. These proteins are mostly expressed in skeletal muscle myotubes, while myoblasts have little or no expression of MHCs.

The purpose of this experiment was to see whether the myotubes from T2D and N-D subjects were fully differentiated. We first conducted a pilot experiment with pooled cell samples of T2D and N-D subjects, to confirm greater expression of MHC in myotubes vs. myoblast, and also to get an indicator of the differentiation capacity in the two donor groups.

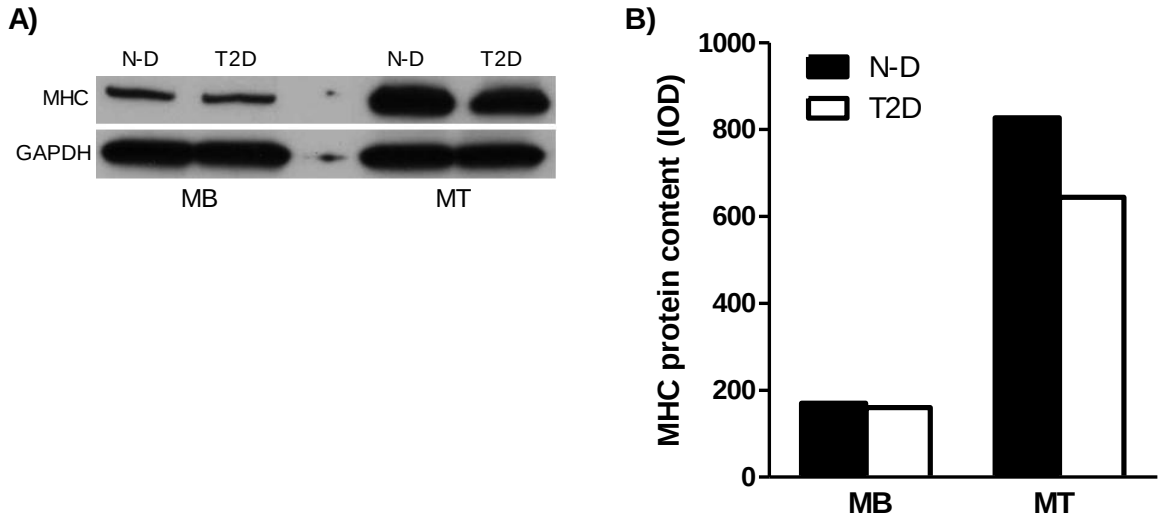

Figure 3.11: Expression of MHC content in human skeletal muscle cells. Myoblasts (MB) and differentiated myotubes (MT) were established from 4 obese type 2 diabetic (T2D) subjects and 4 lean, healthy control subjects (N-D). **A)** Western immunoblot of pooled samples. 25 µg protein of pooled sample were analyzed on a 4-15 % polyacrylamide gel. Primary antibodies; MF20 mouse anti-myosin antibody from Hybridoma Bank at 1:500, 4 °C over night, Abcam mouse anti-GAPDH antibody at 1:1000, 4 °C over night. Secondary antibody; Santa Cruz goat anti-mouse-HRP at 1:10 000, room temperature 1 hour, 10 seconds exposures. **B)** Optical density plot of MHC content in skeletal muscle of T2D and N-D subjects. Values were normalized to GAPDH.

The results showed an increase in MHC protein content from myoblasts to myotubes (figure 3.11 A), as expected. There was no difference in the protein content for the myoblasts, while there seemed to be a lower MHC content in T2D myotubes compared to the control group (figure 3.11 B). There was only one data point for each measurement in this experiment, since the samples were pooled.

After seeing the result of the pilot experiment, we chose to run a 2nd Western immunoblot experiment where we looked at the MHC content in each individual donor in myotubes established from T2D and N-D subjects. The purpose of this experiment was to see whether we could detect a lower MHC content in T2D myotubes compared to the control group, after seeing a trend towards this result in the pilot experiment.

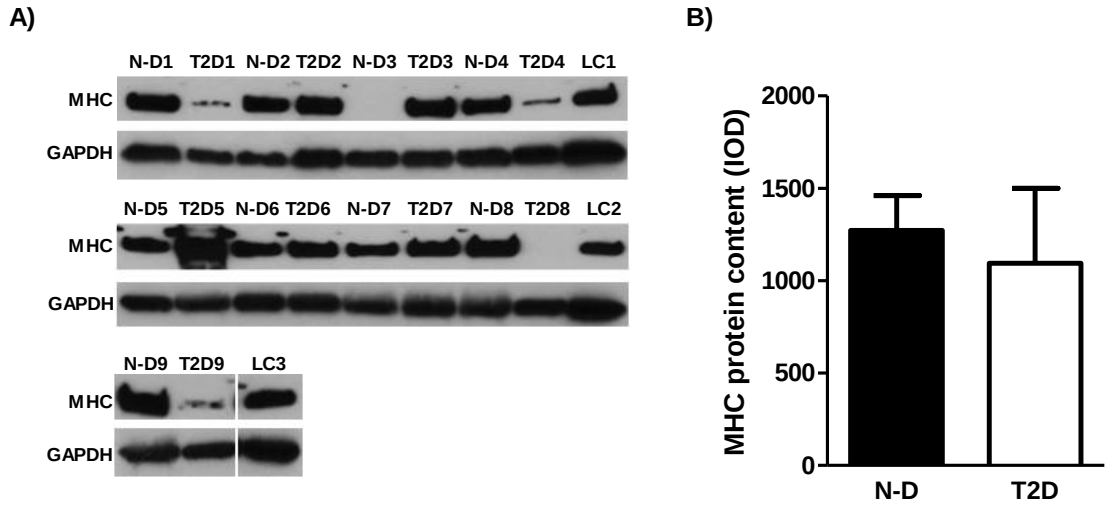

Figure 3.12: Expression of MHC content in human myotubes. Myotubes were established from 9 obese type 2 diabetic (T2D) subjects and 9 lean, healthy control subjects (N-D). **A)** Western immunoblot of individual samples. 25 µg protein of each sample was analyzed on a 4-15 % polyacrylamide gel. Primary antibodies: MF20 mouse anti-myosin antibody from Hybridoma Bank at 1:500, 4 °C over night, Abcam mouse anti-GAPDH antibody at 1:1000, 4 °C over night. Secondary antibody: Santa Cruz goat anti-mouse-HRP at 1:10 000, room temperature 1 hour, 10 seconds exposures. **B)** Optical density plot of MHC protein content in myotubes from T2D and N-D subjects. Values were normalized to GAPDH. All data are given as mean ± S.E.M, and the Mann-Whitney test was applied for comparison of the two donor groups.

Based on the pilot experiment, we expected to see a lower MHC content in the T2D myotubes compared to the control group. The results, however, did not show any significant difference between the two donor groups (figure 3.12 B). The protein content in the N-D myotubes was relatively consistent, while the protein content of the T2D myotubes were more variable (figure 3.12 A). The immunoblot showed one clear outlier in each donor group (N-D3 and T2D5), which may have affected the outcome of the results.

After statistical analysis, we chose to remove the two outliers (N-D3 and T2D5) (figure 3.13 A) and plot the data again. The results showed a significantly lower MHC content in T2D myotubes compared to the control group (figure 3.13 B).

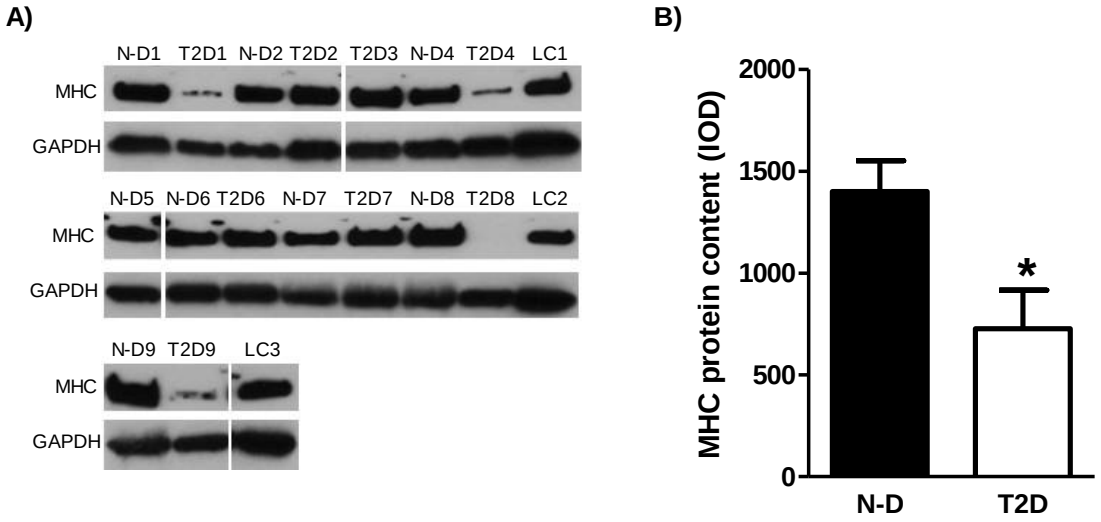

Figure 3.13: Expression of MHC content in human myotubes. A) Western immunoblot with removal of outliers N-D3 and T2D5. **B)** Optical density plot of MHC protein content in myotubes from T2D (n = 8) and N-D (n = 8). All data are given as mean ± S.E.M. *P<0.05 vs. N-D cells

4 Discussion

Metabolic flexibility is characterized by the muscle cells ability to switch from lipid oxidation during fasting to glucose oxidation after a meal. Reduced flexibility, or *metabolic inflexibility*, often occurs with insulin resistance, T2D and obesity[32, 34]. Several studies have shown that individuals with these conditions have a lower mitochondrial number and activity[9, 66]. It has also been suggested that accumulation of lipid in skeletal muscle (intramyocellular lipid, IMCL) and lipid intermediates may be contributing factors to the development of insulin resistance, after observing a reduced muscle fatty acid oxidation in insulin resistant individuals[15]. Taken together, these findings have led to the hypothesis that mitochondrial dysfunction may be driving impaired fatty acid oxidation and consequently lipid accumulation and development of insulin resistance[9].

The present study was undertaken to examine the metabolic properties of skeletal muscle cells from T2D and N-D subjects by looking at the mitochondrial respiration and glycolysis. It was also of interest to determine the mitochondrial content and mass, content of OXPHOS complexes and ATP concentration. The primary findings of this study were that: (1) mitochondrial respiration and glycolysis were substantially impaired in skeletal muscle cells from type 2 diabetic subjects when values were normalized for cellular DNA content (expressed as OCR/µg DNA and ECAR/µg DNA, respectively); that (2) there was no difference in mitochondrial mass or content between cells from the two donor groups, nor was there a difference in the complexes of the electron transport chain (ETC) and the ATP synthase; and that (3) myosin heavy chain (MHC) protein content was significantly lower in T2D myotubes compared with N-D myotubes.

4.1 Metabolic properties of muscle cells from type 2 diabetic and non-diabetic subjects

The VO_{2max} is considered the gold standard for *in vivo* measurements of maximal oxygen consumption. *In vivo* methods are often time consuming and expensive and it is, therefore, often desirable to develop *in vitro* models to perform the same measurements. Human satellite cell cultures are excellent tools for studying metabolic properties *in vitro*, as studies have shown that the diabetic phenotype is conserved in cell cultures established from T2D subjects[38, 39]. Several studies have demonstrated a positive correlation between insulin sensitivity and VO_{2max}[67]. Kennedy et al[68] showed that T2D patients had higher fasting plasma glucose and HbA_{1c} concentrations together with lower VO_{2max} compared to the control subjects. If we can relate *in vivo* findings to *in vitro* experiments, we would expect the OCR of muscle cells from T2D subjects to be lower than the OCR of cells from the control group (non-diabetic subjects).

Assessment of mitochondrial respiration showed a significantly lower OCR in T2D cells compared with cells from non-diabetic subjects. This may be explained by: (1) lower ATP demand in T2D subjects. This would result in less H^+ going through the ATP synthase and less electron flow through the ETC, which in turn would lead to less need for O_2, i.e. lower oxygen consumption, (2) increased coupling between the ETC and OXPHOS. With increased coupling between these two processes, most of the H^+ would go through the ATP synthase, rather than being "lost" to uncoupling proteins and heat production, (3) or both. To assess which of these processes that come into play it would be necessary to make measurements of the ATP production. A lower ATP demand would lead to lower ATP production, while an increased coupling between the ETC and OXPHOS would not necessarily lead to lower ATP production, unless there also is a lower ATP demand.

One can also argue that the lower OCR, observed in cell from T2D subjects, is due to less metabolic activity (i.e. ion pumps and protein synthesis). This would lead to lower ATP demand and consequently lower OCR. However, if the T2D cells have less metabolic activity compared to the control group, one would also expect to see a lower mitochondrial content in this group, which was not the case in our experiments (see figure 3.6 & 3.7).

The rate of extracellular acidification (ECAR) was also significantly lower in cells from T2D subjects compared to the control group. This may be explained by an impaired ability to transport and/or oxidize available glucose in these subjects. GLUT4 translocation is considered to be the major mechanism responsible for the increased rate of glucose transport after insulin or exercise stimulation, and several studies have suggested a reduced translocation of GLUT4 to the plasma membrane in insulin resistant subjects [69-71]. There have also been studies reporting impaired glucose oxidation in T2D subjects. Gaster and Beck-Nielsen[72] showed that baseline glucose oxidation remained unchanged, while the insulin stimulated glucose oxidation was significantly reduced in myotubes established from obese T2D subjects compared to myotubes established from obese control subjects.

Addition of oligomycin led to a drop in OCR due to blocking of the ATP synthase. Blocking of this enzyme will lead to an increase in the glycolytic flux as the cells attempt to recover the mitochondrial ATP loss. We, therefore, expected a negative change in pH from baseline measurements. Interestingly, ECAR measures did not show a change in the myoblasts pH, while the myotubes had a negative pH change from baseline measurements. The drop in OCR in addition to the increased glycolytic flux seen in the myotubes indicated a switch from mitochondrial respiration to glycolysis.

Addition of FCCP will lead to a collapse of the membrane potential across the inner mitochondrial membrane, due to complete hydrogen permeability. This will in turn lead to rapid consumption of energy without the generation of ATP. We, therefore, expected an increase in OCR and ECAR, OCR due to uncoupling and ECAR due to the cells attempt to maintain their energy balance by using glycolysis to generate ATP. The results showed an increase in OCR in both donor groups. We also observed a significantly lower OCR in T2D myotubes after addition of FCCP compared to the control group, indicating a lower potential for maximal oxygen consumption in these cells. These results are consistent with other studies showing that maximal respiration through ETC and FCCP-driven maximal O_2 consumption (i.e. respiration) were significantly decreased in T2D subjects compared with an obese control group[66, 73]. The ECAR results, however, did not show an increase for either of the donor groups.

4.2 Mitochondrial measurements

As mentioned earlier, several researchers have proposed a role for mitochondrial dysfunction in human skeletal muscle of insulin resistant subjects, but whether this is caused by lower mitochondrial content, functional impairment of mitochondria, or both, is still unknown. To address this issue we measured the mitochondrial DNA content (mtDNA), mitochondrial mass and OXPHOS content in skeletal muscle cells from T2D and N-D subjects.

Assessment of mtDNA is regarded as a quantitative index of mitochondrial content in tissue and skeletal muscle[74]. Our experiments did not show any differences in mtDNA between myoblasts and myotubes from T2D and N-D subjects, suggesting that muscle cells from these two groups have similar mitochondrial number. Other studies, however, have found a reduced mtDNA content in skeletal muscle of obese and T2D compared to a lean control group[75], moreover it has been demonstrated that mtDNA content was inversely correlated with BMI[67].

In a study by Kelley *et al*[45] decreased ETC activity was observed in T2D and obese subjects compared with a lean control group. However, when ETC activity was correlated for mitochondrial content, it did not differ significantly across the groups. These findings were supported by a study conducted by Boushel *et al*[76], where they showed that T2D patients had a significantly lower O_2 flux compared with the control group, but that this difference disappeared when the O_2 flux was corrected for mtDNA. These studies implicate a greater role of mitochondrial content, rather than function in mitochondrial dysfunction. A study conducted by Gaster et al[77], however, has later shown that there were no differences in mitochondrial mass between myotubes established from lean, obese and obese T2D subjects. Moreover, Corpeleijn et al[78] showed that mitochondrial mass did not differ between myotubes established from obese T2D subjects and myotubes established from a lean, healthy control group, after a 48 hour treatment with oleic acid. These results are consistent with our mitotracker experiments, showing no difference in mitochondrial mass between T2D myotubes and cells from the control group.

The complexes of the electron transport chain and the ATP synthase (OXPHOS complexes) are essential to mitochondrial respiration, and it was therefore of interest to measure the

protein content of these complexes. Our experiments did not detect any differences between T2D and N-D myotubes in either of the complexes.

Taken together, these findings suggest that the reduction in OCR seen in T2D cells may not be explained by a reduced number of mitochondria or their content of OXPHOS complexes, but rather by an impaired function of the mitochondria.

4.3 ATP concentration

ATP measurements were conducted on cell lysate and live cells established from T2D and N-D subjects. There was no significant difference in ATP concentration between the two donor groups. Our observation of a similar ATP concentration in cells established from T2D and N-D subjects is in line with a study conducted by Gaster et al[77], who showed that there were no differences in ATP concentration in myotubes established from lean, obese and obese T2D subjects.

The limitation of this experiment is that the ATP concentration only was measured at a given time point under non-modulated conditions. The changes in ATP turnover increases and decreases, dependent on the energy demand. The ATP concentration is, however, kept on a homeostatic level, and it is uncommon to observe changes in the ATP concentration[79]. It would, therefore, have been of greater interest to measure the ATP turnover or production rate (e.g. under insulin stimulated conditions), in order to identify possible differences between cells from T2D and N-D subjects.

Minet and Gaster[80] have recently conducted a study measuring the ATP production in isolated mitochondria from myotubes established from lean, obese and T2D subjects. The results showed that the ATP synthesis rate in diabetic mitochondria was significantly impaired, compared to mitochondria established from lean subjects, during ATP utilization (by the hexokinase reaction). Assessment of ATP production rate at baseline or during acute insulin stimulation did not differ significantly between groups. However, Stump et al [81] have found that insulin infusion for longer than 4 hours, increased ATP production in

mitochondria isolated from muscle of healthy subjects, whereas in individuals with T2D, no effect of insulin infusion was observed.

4.4 Differentiation capacity

Lastly, it was also of interest to examine whether the reduction in OCR seen in T2D cells could be explained by an impaired differentiation capacity of myoblasts from these subjects. To address this issue, a marker for differentiation capacity, MHC, was measured in T2D myotubes and compared with myotubes from the control group. MHC was chosen as the differentiation marker; as previous studies have shown that myotubes express significant amounts of MHCs, while myoblasts express extremely low levels of this protein[43].

Initially, the cells were grown in growth medium until ~80 % confluence. Differentiation was induced by switching to differentiation medium, free of added growth factors and only 2% FBS. FBS contains a mixture of growth factors, hormones, albumin, transferrin, protease inhibitors etc, and it is added to the medium to mimic *in vivo* conditions. By removing the growth factors and reducing the FBS the cells are forced to undergo differentiation[40].

The results showed a lower amount of MHC in T2D cells compared to cells from the control group, which may imply an impaired differentiation capacity. It could also indicate a slower differentiation process of these cells. It is, however, impossible to draw any conclusion based on one data point, and further analysis of other proteins and genes essential for the differentiation process (ex; myogenin, MyoD etc) are necessary, to confirm or disprove this hypothesis. It would also be of interest to conduct imaging experiments on cells from the two donor groups, to get a quantitative as well as a visual picture of their differentiation capacity.

5 Conclusion

In the current study we examined the metabolic properties of myoblasts and myotubes established from T2D and N-D subjects. Our data suggest that T2D skeletal muscle cells have a reduced respiratory capacity compared to cells from the control group. Assessment of mitochondrial mass and content, in addition to OXPHOS content did not show any significant difference between myotubes form the two donor groups. Taken together, these observations support the hypothesis of a mitochondrial dysfunction rather than a decreased amount of mitochondria in skeletal muscle from T2D subjects.

In the study we also observed a lower MHC content in myotubes from T2D subjects, compared with myotubes from the control group, which may imply an impaired differentiation capacity of cells established from these subjects. It is therefore difficult to conclude whether the reduced OCR seen in T2D cells is caused by the possible mitochondrial dysfunction or simply because T2D muscle cells were less differentiated than the N-D cells. It is, therefore, necessary to carry out experiments that accounts for the possible impairment in differentiation capacity of T2D cells before we can draw a conclusion.

Lastly, there were two main drawbacks of this study, which may have affected the outcome of the results. First of all the study groups were not matched for age or BMI, which makes it difficult to determine whether differences seen between cells from the two donor groups are caused by T2D, age, obesity or by a combination of these conditions. Secondly, the number of participants was relatively small (n = 5-10 in each group), making it difficult to detect possible differences. Further research with better matched donor groups and a larger n number is, therefore, necessary.

6 References

1. Alberti, K., P. Zimmet, and W. Consultation, *Definition, diagnosis and classification of diabetes mellitus and its complications. Part 1: diagnosis and classification of diabetes mellitus. Provisional report of a WHO consultation.* Diabetic medicine, 1998. **15**(7): p. 539-553.
2. WHO, *World Health Organization: Diabetes programme.* 2009: p. http://www.who.int/diabetes/facts/en/index.html.
3. Younis, N., H. Soran, and S. Farook, *The prevention of type 2 diabetes mellitus: recent advances.* QJM, 2004. **97**(7): p. 451.
4. *Norsk legemiddelhåndbok.* 2010.
5. Stumvoll, M., B. Goldstein, and T. van Haeften, *Type 2 diabetes: principles of pathogenesis and therapy.* The Lancet, 2005. **365**(9467): p. 1333-1346.
6. Leahy, J., *Pathogenesis of type 2 diabetes mellitus.* Type 2 Diabetes Mellitus, 2008: p. 17-33.
7. Jin, W. and M. Patti, *Genetic determinants and molecular pathways in the pathogenesis of Type 2 diabetes.* Clinical Science, 2009. **116**: p. 99-111.
8. Hegarty, B., et al., *The role of intramuscular lipid in insulin resistance.* Acta Physiologica Scandinavica, 2003. **178**(4): p. 373-383.
9. Savage, D., K. Petersen, and G. Shulman, *Disordered lipid metabolism and the pathogenesis of insulin resistance.* Physiological reviews, 2007. **87**(2): p. 507.
10. Hawley, J.A. and J.O. Holloszy, *Exercise: it's the real thing!* Nutrition reviews, 2009. **67**(3): p. 172-178.
11. Frederiksen, C., et al., *Transcriptional profiling of myotubes from patients with type 2 diabetes: no evidence for a primary defect in oxidative phosphorylation genes.* Diabetologia, 2008. **51**(11): p. 2068-2077.
12. Gaster, M., et al., *Reduced Lipid Oxidation in Skeletal Muscle From Type 2 Diabetic Subjects May Be of Genetic Origin.* Diabetes, 2004. **53**(3): p. 542.
13. Samuel, V.T., K.F. Petersen, and G.I. Shulman, *Lipid-induced insulin resistance: unravelling the mechanism.* The Lancet, 2010. **375**(9733): p. 2267-2277.
14. Krssak, M. and M. Roden, *The role of lipid accumulation in liver and muscle for insulin resistance and type 2 diabetes mellitus in humans.* Reviews in Endocrine & Metabolic Disorders, 2004. **5**(2): p. 127-134.
15. Kelley, D., et al., *Skeletal muscle fatty acid metabolism in association with insulin resistance, obesity, and weight loss.* American Journal of Physiology- Endocrinology And Metabolism, 1999. **277**(6): p. E1130.
16. Turner, N. and L. Heilbronn, *Is mitochondrial dysfunction a cause of insulin resistance?* Trends in Endocrinology & Metabolism, 2008. **19**(9): p. 324-330.
17. Tremblay, F., M. Dubois, and A. Marette, *Regulation of GLUT4 traffic and function by insulin and contraction in skeletal muscle.* Front Biosci, 2003. **8**: p. d1072-d1084.
18. Lowell, B. and G. Shulman, *Mitochondrial dysfunction and type 2 diabetes.* Science, 2005. **307**(5708): p. 384.
19. Zurlo, F., et al., *Skeletal muscle metabolism is a major determinant of resting energy expenditure.* Journal of Clinical Investigation, 1990. **86**(5): p. 1423.
20. Galgani, J., C. Moro, and E. Ravussin, *Metabolic flexibility and insulin resistance.* American Journal of Physiology- Endocrinology And Metabolism, 2008. **295**(5): p. E1009.

21. Gould, G. and G. Holman, *The glucose transporter family: structure, function and tissue-specific expression.* Biochemical Journal, 1993. **295**(Pt 2): p. 329.
22. Saltiel, A.R. and C.R. Kahn, *Insulin signalling and the regulation of glucose and lipid metabolism.* Nature, 2001. **414**(6865): p. 799-806.
23. Garvey, W., et al., *Gene expression of GLUT4 in skeletal muscle from insulin-resistant patients with obesity, IGT, GDM, and NIDDM.* Diabetes, 1992. **41**(4): p. 465.
24. Björnholm, M., et al., *Insulin receptor substrate-1 phosphorylation and phosphatidylinositol 3-kinase activity in skeletal muscle from NIDDM subjects after in vivo insulin stimulation.* Diabetes, 1997. **46**(3): p. 524.
25. Goodyear, L., et al., *Insulin receptor phosphorylation, insulin receptor substrate-1 phosphorylation, and phosphatidylinositol 3-kinase activity are decreased in intact skeletal muscle strips from obese subjects.* Journal of Clinical Investigation, 1995. **95**(5): p. 2195.
26. Olav Sand, Ø.V.S., Egil Haug, *Menneskets Fysiologi*. 2001, Gyldendal Norsk Forlag AS: Oslo.
27. Alberts, B., et al., *Essential cell biology*. Second edition ed. 2004, New York: Garland Science.
28. Aas, V., et al., *Lipid metabolism in human skeletal muscle cells: effects of palmitate and chronic hyperglycaemia.* Acta Physiologica Scandinavica, 2005. **183**(1): p. 31-41.
29. Kelley, D. and J. Simoneau, *Impaired free fatty acid utilization by skeletal muscle in non-insulin-dependent diabetes mellitus.* Journal of Clinical Investigation, 1994. **94**(6): p. 2349.
30. Mensink, M., et al., *Plasma free fatty acid uptake and oxidation are already diminished in subjects at high risk for developing type 2 diabetes.* Diabetes, 2001. **50**(11): p. 2548.
31. Krssak, M., et al., *Intramyocellular lipid concentrations are correlated with insulin sensitivity in humans: a 1H NMR spectroscopy study.* Diabetologia, 1999. **42**(1): p. 113-116.
32. Kelley, D., *Skeletal muscle fat oxidation: timing and flexibility are everything.* Journal of Clinical Investigation, 2005. **115**(7): p. 1699-1702.
33. Storlien, L., N. Oakes, and D. Kelley, *Metabolic flexibility.* Proceedings of the Nutrition Society, 2004. **63**(02): p. 363-368.
34. Kelley, D.E. and L.J. Mandarino, *Fuel selection in human skeletal muscle in insulin resistance: a reexamination.* Diabetes, 2000. **49**(5): p. 677.
35. Contaldoa, M.M.L.S.F. and F. Pasanisia, *Fasting respiratory quotient as a predictor of long-term weight changes in non-obese women.* Ann Nutr Metab, 2004. **48**: p. 189-192.
36. Zurlo, F., et al., *Low ratio of fat to carbohydrate oxidation as predictor of weight gain: study of 24-h RQ.* American Journal of Physiology-Endocrinology And Metabolism, 1990. **259**(5): p. E650.
37. Colberg, S.R., et al., *Skeletal muscle utilization of free fatty acids in women with visceral obesity.* Journal of Clinical Investigation, 1995. **95**(4): p. 1846.
38. Gaster, M., et al., *The Diabetic Phenotype Is Conserved in Myotubes Established From Diabetic Subjects.* Diabetes, 2002. **51**(4): p. 921.
39. Ciaraldi, T., et al., *Glucose transport in cultured human skeletal muscle cells. Regulation by insulin and glucose in nondiabetic and non-insulin-dependent diabetes mellitus subjects.* Journal of Clinical Investigation, 1995. **96**(6): p. 2820.

40. Gilbert, S.F., *Developmental Biology*. Sixth edition ed. 2000, Massachusetts: Sunderland (MA).
41. Zammit, P., T. Partridge, and Z. Yablonka-Reuveni, *The skeletal muscle satellite cell: the stem cell that came in from the cold.* Journal of Histochemistry and Cytochemistry, 2006. **54**(11): p. 1177.
42. Sabourin, L. and M. Rudnicki, *The molecular regulation of myogenesis.* Clinical genetics, 2000. **57**(1): p. 16-25.
43. Remels, A., et al., *Regulation of mitochondrial biogenesis during myogenesis.* Molecular and cellular endocrinology, 2010. **315**(1-2): p. 113-120.
44. Maechler, P. and C. Wollheim, *Mitochondrial function in normal and diabetic -cells.* Nature, 2001. **414**(6865): p. 807-812.
45. Kelley, D., et al., *Dysfunction of mitochondria in human skeletal muscle in type 2 diabetes.* Diabetes, 2002. **51**(10): p. 2944.
46. Brehm, A., et al., *Increased lipid availability impairs insulin-stimulated ATP synthesis in human skeletal muscle.* Diabetes, 2006. **55**(1): p. 136.
47. Petersen, K., et al., *Impaired mitochondrial activity in the insulin-resistant offspring of patients with type 2 diabetes.* New England Journal of Medicine, 2004. **350**(7): p. 664.
48. Simoneau, J. and D. Kelley, *Altered glycolytic and oxidative capacities of skeletal muscle contribute to insulin resistance in NIDDM.* Journal of Applied Physiology, 1997. **83**(1): p. 166.
49. Hickner, R., et al., *Lipid oxidation is reduced in obese human skeletal muscle.* American Journal of Physiology, 2000. **279**(5 (1)): p. e1039-e1044.
50. Patti, M.E., et al., *Coordinated reduction of genes of oxidative metabolism in humans with insulin resistance and diabetes: potential role of PGC1 and NRF1.* Proceedings of the National Academy of Sciences of the United States of America, 2003. **100**(14): p. 8466.
51. Kadenbach, B., *Intrinsic and extrinsic uncoupling of oxidative phosphorylation* 1.* Biochimica et Biophysica Acta (BBA)-Bioenergetics, 2003. **1604**(2): p. 77-94.
52. Belogrudov, G.I., J.M. Tomich, and Y. Hatefi, *ATP synthase complex.* Journal of Biological Chemistry, 1995. **270**(5): p. 2053.
53. Boyer, P.D., *The ATP synthase--a splendid molecular machine.* Annual review of biochemistry, 1997. **66**: p. 717.
54. Panek, J. and N. Jain, *Total Synthesis of Rutamycin B and Oligomycin C.* J. Org. Chem, 2001. **66**(8): p. 2747-2756.
55. Shchepina, L., et al., *Oligomycin, inhibitor of the F 0 part of H+-ATP-synthase, suppresses the TNF-induced apoptosis.* Oncogene, 2002. **21**(53): p. 8149-8157.
56. Park, K., et al., *FCCP depolarizes plasma membrane potential by activating proton and Na+ currents in bovine aortic endothelial cells.* Pflügers Archiv European Journal of Physiology, 2002. **443**(3): p. 344-352.
57. Benz, R. and S. McLaughlin, *The molecular mechanism of action of the proton ionophore FCCP (carbonylcyanide p-trifluoromethoxyphenylhydrazone).* Biophysical Journal, 1983. **41**(3): p. 381-398.
58. Terada, H., *Uncouplers of oxidative phosphorylation.* Environmental Health Perspectives, 1990. **87**: p. 213.
59. Berggren, J., C. Tanner, and J. Houmard, *Primary cell cultures in the study of human muscle metabolism.* Exercise and sport sciences reviews, 2007. **35**(2): p. 56.

60. Ferrick, D.A., A. Neilson, and C. Beeson, *Advances in measuring cellular bioenergetics using extracellular flux.* Drug discovery today, 2008. **13**(5-6): p. 268-274.
61. Wu, M., et al., *Multiparameter metabolic analysis reveals a close link between attenuated mitochondrial bioenergetic function and enhanced glycolysis dependency in human tumor cells.* American Journal of Physiology- Cell Physiology, 2007. **292**(1): p. C125.
62. Bradford, M., *A rapid and sensitive method for the quantitation of microgram quantities of protein utilizing the principle of protein-dye binding.* Analytical biochemistry, 1976. **72**(1-2): p. 248-254.
63. Luo, J. and L. Luo, *American Ginseng Stimulates Insulin Production and Prevents Apoptosis through Regulation of Uncoupling Protein-2 in Cultured{beta} Cells.* Evidence-based Complementary and Alternative Medicine, 2006. **3**(3): p. 365.
64. Cohen, A., *Xylenol Blue: And its proposed use as a new and improved indicator in Chemical and Biochemical work.* Biochemical Journal, 1922. **16**(1): p. 31.
65. Dvoriantchikova, G., et al., *Liposome-delivered ATP effectively protects the retina against ischemia-reperfusion injury.* Molecular Vision, 2010. **16**: p. 2882.
66. Mogensen, M., et al., *Mitochondrial respiration is decreased in skeletal muscle of patients with type 2 diabetes.* Diabetes, 2007. **56**(6): p. 1592.
67. Ukropcova, B., et al., *Family history of diabetes links impaired substrate switching and reduced mitochondrial content in skeletal muscle.* Diabetes, 2007. **56**(3): p. 720.
68. Kennedy, J.W., et al., *Acute exercise induces GLUT4 translocation in skeletal muscle of normal human subjects and subjects with type 2 diabetes.* Diabetes, 1999. **48**(5): p. 1192.
69. Zierath, J., et al., *Insulin action on glucose transport and plasma membrane GLUT4 content in skeletal muscle from patients with NIDDM.* Diabetologia, 1996. **39**(10): p. 1180-1189.
70. Garvey, W.T., et al., *Evidence for defects in the trafficking and translocation of GLUT4 glucose transporters in skeletal muscle as a cause of human insulin resistance.* Journal of Clinical Investigation, 1998. **101**(11): p. 2377.
71. Kelley, D.E., et al., *The effect of non-insulin-dependent diabetes mellitus and obesity on glucose transport and phosphorylation in skeletal muscle.* Journal of Clinical Investigation, 1996. **97**(12): p. 2705.
72. Gaster, M. and H. Beck-Nielsen, *The reduced insulin-mediated glucose oxidation in skeletal muscle from type 2 diabetic subjects may be of genetic origin--evidence from cultured myotubes.* Biochimica et Biophysica Acta (BBA)-Molecular Basis of Disease, 2004. **1690**(1): p. 85-91.
73. Phielix, E., et al., *Lower intrinsic ADP-stimulated mitochondrial respiration underlies in vivo mitochondrial dysfunction in muscle of male type 2 diabetic patients.* Diabetes, 2008. **57**(11): p. 2943.
74. Miller, F.J., et al., *Precise determination of mitochondrial DNA copy number in human skeletal and cardiac muscle by a PCR based assay: lack of change of copy number with age.* Nucleic acids research, 2003. **31**(11): p. e61.
75. Ritov, V.B., et al., *Deficiency of subsarcolemmal mitochondria in obesity and type 2 diabetes.* Diabetes, 2005. **54**(1): p. 8.
76. Boushel, R., et al., *Patients with type 2 diabetes have normal mitochondrial function in skeletal muscle.* Diabetologia, 2007. **50**(4): p. 790-796.
77. Gaster, M., *Mitochondrial mass is inversely correlated to complete lipid oxidation in human myotubes.* Biochemical and Biophysical Research Communications, 2010.

78. Corpeleijn, E., et al., *Oxidation of intramyocellular lipids is dependent on mitochondrial function and the availability of extracellular fatty acids.* American Journal of Physiology-Endocrinology And Metabolism, 2010. **299**(1): p. E14.
79. Hochachka, P. and G. McClelland, *Cellular metabolic homeostasis during large-scale change in ATP turnover rates in muscles.* The Journal of experimental biology, 1997. **200**(Pt 2): p. 381.
80. Minet, A.D. and M. Gaster, *ATP synthesis is impaired in isolated mitochondria from myotubes established from type 2 diabetic subjects.* Biochemical and Biophysical Research Communications, 2010.
81. Stump, C., et al., *Effect of insulin on human skeletal muscle mitochondrial ATP production, protein synthesis, and mRNA transcripts.* Proceedings of the National Academy of Sciences of the United States of America, 2003. **100**(13): p. 7996.

Appendix

Different medium

Cell culturing

Growth medium

450 ml	DMEM Low glucose
50 ml	FBS
3 ml	7 % BSA
5 ml	Fetuin in HBSS
500 µl	huEGF
500 µl	Dexametasone
5 ml	Antibiotic/antimycotic solution

Differentiation medium

480 ml	MEM alpha
10 ml	FBS
5 ml	Fetuin in HBSS
5 ml	Antibiotic/antimycotic solution

Western immunoblotting

Running buffer

100 ml	10X Tris/Glycine/SDS buffer
900 ml	ddH_2O

Transfer buffer

6,06 g	Trizma® Base
28,8 g	Glycine for electrophoresis minimum 99 %
400 ml	Methanol
1600 ml	ddH_2O

Wash buffer ECL

200 ml	10X DPBS
1 ml	Tween 20
1800 ml	ddH_2O

Wash buffer Odyssey

200 ml	10X TBS
2 ml	Tween 20
1800 ml	ddH_2O

Blocking buffer ECL

50 ml	Wash buffer ECL
2,5 g	Blotting grade blocker non-fat dry milk

Blocking buffer Odyssey

10 ml	10X TBS
90 ml	ddH_2O
100 ml	Odyssey® blocking buffer

Antibodies ECL

40 ml Blocking buffer ECL

Primary	1:500	MF20 mouse anti-myosin
Primary	1:1000	Mouse anti-GAPDH
Secondary	1:10 000	Goat-anti-mouse IgG HRP

Antibodies Odyssey

40 ml Blocking buffer Odyssey

Primary	1:500	MS601 mouse anti-human OXPHOS
Primary	1:1000	Mouse anti-human GAPDH
Secondary	1:10 000	Goat anti-mouse IgG Alexa Fluor 680

Substrate for developing ECL

5 ml	Lumigen™ PS-3 detection reagent, Solution A
100 µl	Lumigen™ PS-3 detection reagent, Solution B

Real Time PCR

18 S

1500 µl	TaqMan 2X Universal PCR Master Mix
150 µl	18S
450 µl	Nuclease free water

ND1

1500 µl	TaqMan 2 X Universal PCR Master Mix
180 µl	ND1 Primer F (forward)
180 µl	ND1 Primer R (reverse)
75 µl	ND1 Probe
165 µl	Nuclease free water

ND4

1500 µl	TaqMan 2 X Universal PCR Master Mix
180 µl	ND4 Primer F (forward)
180 µl	ND4 Primer R (reverse)
75 µl	ND4 Probe
165 µl	Nuclease free water

Sequences

ND1 Primer F:	IDT, 5'-CCC TAA AAC CCG CCA CAT CT-3'
ND1 Primer R:	IDT, 5'-GAG CGA TGG TGA GAG CTA AGG-3'
ND1 Probe:	IDT, 5'-FAM-CCA TCA CCC TCT ACA CCG-3'
ND4 Primer F:	IDT, 5'-CCA TTC TCC TCC TAT CCC TCA AC-3'
ND4 Primer R:	IDT, 5-CAC AAT CTG ATG TTT TGG TTA AAC TAT-3'
ND4 Probe:	IDT, 5'-FAM-CCG ACA TCA TTA CCG GGT TTT-3'

Mitotracker

Mitotracker solution A – 1 mM

1 vial	Mitotracker® Green FM
74.4 µl	DMSO

Mitotracker solution B – 100 µM

5 µl	Mitotracker solution A
45 µl	MEM alpha

Mitotracker solution C – 100 nM

10 µl	Mitotracker solution B
10 ml	MEM alpha

Calculations for final concentrations of oligomycin and FCCP

Injections of oligomycin: 75 µl, 50 µM, in 625 µl XF24 assay medium
Final volume after injection: 75 µl + 625 µl = 700 µl

Final concentration of oligomycin in each well of the XF24 cell culture microplate

$50\mu\, mol/l \times 7.5 \times 10^{-5} l = 3.75 \times 10^{-4} \mu mol$

$3.75 \times 10^{-4} \mu mol / 7.0 \times 10^{-4} l = 5.35 \mu mol/l \approx 5.4 \mu M$

Injections of FCCP: 75 µl, 10 µM, in 625 µl XF24 assay medium + 75µl oligomycin
Final volume after injection: 75 µl + 625 µl + 75 µl = 775 µl

Final concentration of FCCP in each well of the XF24 cell culture microplate

$10\mu\, mol/l \times 7.5 \times 10^{-5} l = 7.5 \times 10^{-4} \mu mol$

$7.5 \times 10^{-4} \mu mol / 7.75 \times 10^{-4} l = 0.96\ \mu mol/l \approx 1.0 \mu M$

RNA experiments for gene expression

All preparatory work is completed (RNA extraction, cleaning and purification, and cDNA synthesis). Rt-PCR experiments for gene expression of different markers for differentiation capacity (MyoD and myogenin) still remains.

RNA extraction and quantification

Total RNA was extracted from the cells by using the RNeasy® Mini Kit (QIAGEN). Briefly, the cells were lysed and homogenized in the wells by adding cell lysis buffer (CLB), and then transferred to an Eppendorf tube. Equal volume 70% EtOH was added to each sample to precipitate RNA. The cell suspension was transferred to a centrifugal tube, where the RNA binds directly to the RNeasy column. The column was washed 3 times to remove contaminants and enzyme inhibitors. Extracts were collected in a final volume of 50 µl of elution buffer. RNA samples were quantified and assessed for purity by using a spectrophotometer, ND-100 from NanoDrop®, and then stored at -80°C until further analysis.

Removal of contaminants from RNA samples

RNA samples with 260/230 (measure of organic contamination) and 260/280 (measure of nucleotide concentration and protein contamination) ratios below 1.80 were further processed to achieve ratios above 1.80 necessary for efficient reactions. This was done by using the RNA Clean-Up protocol from Ravussin's lab. Briefly, RNA samples were defrosted on ice before adding 100 % ethanol (2X of volume that RNA was eluted in originally) and 3M sodium acetate, pH = 8 (10 % of volume that RNA was eluted in originally) to each tube. The tubes were then placed at – 20 °C over night.

The next day the tubes were defrosted on ice and spun at 12 000 RCF (4 °C) for 45 minutes. The aspirate was pulled off, and RNA was resuspended in 100 µl of 70 % ethanol. The RNA suspension was then vortex and spun at 7500 RCF (25℃) for 5 minutes. This process was

repeated twice, before pulling off the aspirate again. The dry RNA was centrifuged at 7500 RCF (25℃) for 5 minutes, and any extra aspirate was pulled off. The samples were then incubated at 37℃ for 5 minutes, until all visible ethanol had evaporated. The dry RNA was resuspended in 15 µl of Nuclease Free Water. RNA levels were quantified and assessed for purity by using a spectrophotometer, ND-100 from NanoDrop®, and then stored at -80°C until further analysis.

Making cDNA from RNA - RNA purification

RNA was purified by using Deoxyribonuclease I, Amplification Grade protocol (Invitrogen). Total RNA extracted from the cells, was diluted with nuclease free water to a concentration of 0.0625 ug/ul with end volume of 16 µl. 4 µl of DNase medium was added to each tube following incubation at room temperature for 15 minutes. 2 µl of EDTA was then added to each well to stop the DNase reaction following heating to 65 °C for 10 minutes.

Making cDNA from RNA - cDNA synthesis

cDNA synthesis was performed by using the iScript™ cDNA synthesis Kit protocol (BioRad). 20 µl of cDNA medium was added to each tube. The tubes were incubated at 25 °C for 5 minutes, 42 °C for 30 minutes and then 85 °C for 5 minutes before they were stored at -20 °C until further analysis.

Overview of project